CURVE AND CIRCLE FITTING OF 3D DATA ACQUIRED BY RGB-D SENSOR

YAMONE HLA WIN

M.C.Sc. **FEBRUARY 2019**

CURVE AND CIRCLE FITTING OF 3D DATA ACQUIRED BY RGB-D SENSOR

BY

YAMONE HLA WIN
B.C.Sc.

A Dissertation Submitted in Partial Fulfillment of the Requirements for the Degree of

Master of Computer Science
(M.C.Sc.)

University of Computer Studies, Yangon
FEBRUARY 2019

ACKNOWLEDGEMENTS

I would like to express my respectful gratitude to **Dr. Mie Mie Thet Thwin**, Rector, University of Computer Studies, Yangon, for allowing me to develop this thesis and giving me general guidance during the period of study.

I'm deeply grateful to my supervisor, **Dr. Myint Myint Sein**, Professor, Department of Geographical Information System, University of Computer Studies, Yangon, for her close guidance, helpful advice, numerous invaluable suggestions, patience and support she has provided throughout my time. I consider myself very fortunate for having been able to work with a very considerate and encouraging supervisor like her.

My thanks and respects go to **Dr. Thi Thi Soe Nyunt**, Professor and Head of Faculty of Computer Science, University of Computer Studies, Yangon, for her invaluable guidance and administrative support, as Dean of Master Course, throughout the development of the thesis.

And also I would like to express my gratefulness to **Dr. Kikuhito Kawasue**, Professor, University of Miyazaki, Japan for his suggestions, patience and support while I studied my master thesis in Japan.

I would like to thank **Daw Aye Moh Moh Shwe**, Assistant Lecturer, Department of Language, for her suggestions and help from language point of view.

Thanks are also extended especially to all my teachers, my parents, seniors, friends and staff members of the University of Computer Studies, Yangon for the contribution towards the completion of this thesis.

STATEMENT OF ORIGINALITY

I hereby certify that the work embodies in this thesis is the result of original research and has not been submitted for a higher degree to any other University or Institution.

---------- ----------

Date Yamone Hla Win

ABSTRACT

In robot vision systems, three-dimensional data reconstruction becomes popular to be used in new research procedures. There are different types of depth sensors in industrial applications. These sensors are easy to access the data while capturing. RGB-D sensor obtains the three-dimensional point cloud data from one single shot. Xtion 2 depth sensor detects all point cloud data clearly which can be seen by sensor. Therefore, it is very important to observe the high precision results while using in grasping applications. We developed the curve and circle fitting of 3D data acquired by the sensor. In this system, the 3D point cloud data is examined by curve and circle estimation from sensor. Moreover, the adjusted R-square Regression Model is applied to verify the accuracy results between estimated data and actual data. This system is implemented by using Visual C++ language in Microsoft Visual Studio and using Microsoft Foundation Class (MFC) window form application. In implementation of measurement system, the pig model is used in measurement area.

CONTENTS

LIST OF FIGURES

LISTS OF TABLES

LISTS OF EQUATIONS

CHAPTER 1

INTRODUCTION

In the Computer Vision field, there are several methods that work with primitive shapes to reconstruct incomplete point clouds. Actually, the obtained data where is only cross section positions of measurement objects. All of these cross sections are gone with the shapes of measurement objects. In this case, the primitive shapes of cross section should be a circle or a curve. Therefore, it is not aimed to reconstruct a circle and a curve model using RGB-D sensor. Three-dimensional point cloud data is obtained by the sensor. In this research, the circle and curve fitting approach is used to analyze how well fits the data shapes of point cloud data from RGB-D sensor. Curve model fitting and circle model fitting are popular in robot vision systems because it is very important to consider directly when the objects enter to the camera. Most of the young researchers introduced new robot vision technologies in order to support high precision results.

1.1 Primitive Data Shapes Fitting of Point Cloud Data

A point cloud is a set of vertices in a three-dimensional (3D) coordinate system [13],[22],[23],[24]. These point cloud data are used in industrial applications and robot vision systems.

In recent years, the RGB-D sensor [27] that can detect the three-dimensional point cloud data, has become available. Two major concepts [7], time of flight (ToF) and structured light (SL), are used in RGB-D sensors. Microsoft KINECT is introduced to capture motion or modeling systems, which is developed by Microsoft Cooperation [10],[17],[25]. That Microsoft KINECT [1],[5],[16] becomes very attractive because there is no limitation on the measurement area size since individual 3D point sets recorded from different positions can be combined on the computer. The device is effective for motion and modelling systems, and the obtained data are not sufficiently accurate for industrial applications but are sufficient for agricultural applications.

Machine vision-based weighting of pigs is a non-intrusive and enable us a fast and accurate approach [10],[17]. Since these systems are fixed type system on the

ground, a compact system is desirable to save the space in the pig house. The iterative closet point algorithm is often employed to combine data sets. This algorithm automatically determines the overlapping area between 3D point cloud data sets and constructs a single 3D image.

The automatic measurement system which is composed of RGB-D sensor which is used to obtain three-dimensional data of pig. Weight of pig is one of the vital index for the reasons such as checking their activities, feed requirements and growth rates, health status are need to be monitored in a pig farming. The daily growth rate and nutritional status are appraised by obtaining pig's weight timely [8]. Getting the pig weight is usually obtained by manual or automatics scales. It is laborious operation that required the hard work, to get the weight of pigs using these scales. Generally, the monitor is executed qualitatively by human eye. Accuracy of predicting proper pig weight (around 115 kg) advances to their profitability. Today, the measurement of pig weight is not done in many pig farms, as it requires the hard labor works. In most of the traditional measurements, pigs are used to be moved to weighing device such like a load cell and electronic balance. The entire process costs time consuming and laborious, and it requires at least two stockmen to spend with each pig [4]. Therefore, the development of a simple weight measurement system is required.

In 3D, parametric shapes such as planes, spheres, cylinders and cones can be considered as geometric primitives that are used to explain parts of the 3D point cloud. Such geometric primitives enable the system to add surface information for parts of the object that were not covered by the sensor data. Moreover, exploiting the knowledge about the shape enables to eliminate inaccuracies.

According to this status, the regression model can be used to fit the shapes to a model are fitted to a model. R-squared is a statistic that explains the amount of variations accounted for in the relationship between two (or more) variables. It is called the coefficient of determination, and it is given as the square of a correlation coefficient. It will give some information about the goodness of fit to a model. In regression, the R^2 coefficient of determination is a statistical measure of how well the regression shapes approximates the real data points. 1 R^2 indicated that the regression shapes perfectly fits the data.

In statistical analysis, the adjusted R-squared is the best to estimate the correlation of models with number of predictors in the model correctly. The adjusted

R-squared is a modified version of R-squared that has been adjusted for the number of predictors in the model. The adjusted R-squared increases only if the new term improves the model more than expected by chance. It decreases when a predictors improves the model by less than expected by chance. It can be negative, but it is usually not. It is always lower than the R-squared.

In this system, it is aimed to analyze the accuracy results of curve model fitting and circle model fitting on point cloud data based on RGB-D sensor by applying adjusted R-squared regression model.

1.2 Objectives of the System

The objectives of the system are:

- To study how RGB-D sensor works on model fitting
- To observe the curve model and circle model fitting procedures
- To introduce the handy type system with RGB-D sensor that can get clear depth data in measurement
- To be effective of skillful workers in hard work operation.

The objectives of this study are to develop how well fit the data shapes using the point cloud data.

1.3 Motivation

In robot vision system, it is important that the data are accepted with the shapes using point cloud data. RGB-D sensors are used in measuring the object and detection processes. It is main that how perfect the sensors can fit the data shapes of measurement target. Therefore, the model fitting is applied in estimation of how well the data fit the shapes using point cloud data.

1.4 Organization of the System

This system claims that the results of curve and circle fitting using RGB-D sensor are planned to observe the accuracy results of the approach. The goal of this system is to estimate how well the fitting 3D data shapes of incomplete point cloud data which can support the higher precision using RGB-D sensor for model fitting. This thesis is organized as follows. The outline of this system consists of five chapters.

Chapter 1 introduces about the system. Chapter 2 explains the theoretical background of the system. Chapter 3 describes the study of fitting data of RGB-D sensor. Chapter 4 focuses on the system design and implementation. Chapter 5 presents the conclusion and further extensions of the system.

CHAPTER 2

THEORETICAL BACKGROUND

In computer vision and computer graphics, 3D reconstruction is the process of capturing the shape and appearance of real objects. This process can be accomplished either by active or passive methods [13]. In recent decades, there is an important demand for 3D content for computer graphics, virtual reality and communication, triggering a change in emphasis for the requirements. Many existing systems for constructing 3D models are built around specialized hardware (e.g. stereo rigs) resulting in a high cost, which cannot satisfy the requirement of its new applications. This gap stimulates the use of digital imaging facilities (like a camera). The task of converting multiple 2D images into 3D model consists of a series of processing steps.

2.1 3D Image Reconstruction

The essence of an image is a projection from a 3D scene onto a 2D plane, during which process the depth is lost. The 3D point corresponding to a specific image point is constrained to be on the line of sight. From a single image, it is impossible to determine which point on this line corresponds to the image point. If two images are available, then the position of a 3D point can be found as the intersection of the two projection rays. This process is referred to as triangulation. The key for this process is the relations between multiple views which convey the information that corresponding sets of points must contain some structure and that this structure is related to the poses and the calibration of the camera.

Camera calibration consists of intrinsic and extrinsic parameters, without which at some level no arrangement of algorithms can work. The dotted line between Calibration and Depth determination represents that the camera calibration is usually required for determining depth [11].

Depth determination serves as the most challenging part in the whole process, as it calculates the 3D component missing from any given image – depth. The correspondence of problem and finding matches between two images so the position of the matched elements that can be triangulated in 3D space is the key issue here.

Once multiple depth maps combine to create a final mesh by calculating depth and projecting out of the camera is called registration. Camera calibration will be used to identify where the many meshes created by depth maps can be combined together to develop a larger one, providing more than one view for observation.

There are two types for 3D image reconstruction: active methods and passive methods.

2.1.1 Active Methods

Active methods, i.e. range data methods, given the depth map, reconstruct the 3D profile by numerical approximation approach and build the object in scenario based on model [11]. These methods actively interfere with the reconstructed object, either mechanically or laser methodology, in order to acquire the depth map, e.g. structured light, laser range finder and other active sensing techniques. Some applicable radiometric methods emit radiance towards the object and then measure its reflected part. Examples range from moving light sources, colored visible light, time-of-flight lasers to microwaves or ultrasound.

2.1.2 Passive Methods

Passive methods of 3D reconstruction do not interfere with the reconstructed object; they only use a sensor to measure the radiance reflected or emitted by the object's surface to infer its 3D structure through image understanding [13]. Typically, the sensor is an image sensor in a camera sensitive to visible light and the input to the method is a set of digital images (one, two or more) or video. By comparison to active methods, passive methods can be applied to a wider range of situations.

2.2 Cross Section

A cross section is non-empty of solid object in three-dimensional spaces with a plane section, or the incomplete position of higher-dimensional spaces in Mathematics, Geometry and Science. Cutting an object into many divisions creates many parallel cross sections. Each cross section in three-dimensional space is parallel to each other, that is , parallel to planes determined by these cross section’s axes, is referred to contour line, for example, if a plane cuts through mountains of raised-relief map parallel showing points on the surface of the mountains of equal elevation. In

technical drawing of a cross-section, it is a projection of an object into a plane that intersects the objects and it is a common tool used to depict the internal arrangement of a three-dimensional object in two dimensions.

Cross section for cylinder shapes of objects is shown in figure 2.1. A related concept is a plane section, which is the curve of intersection of a plane with a surface. Thus, a plane section is the boundary of a cross-section of a solid in a cutting plane.

If a surface in a three-dimensional space is defined by a function of two variables, i.e., z = f(x, y), the plane sections by cutting planes that are parallel to a coordinate plane (a plane determined by two coordinate axes). More specifically, cutting planes with equations of the form z = k (planes parallel to the x y-plane) produces plane sections that are often called contour lines in application areas.

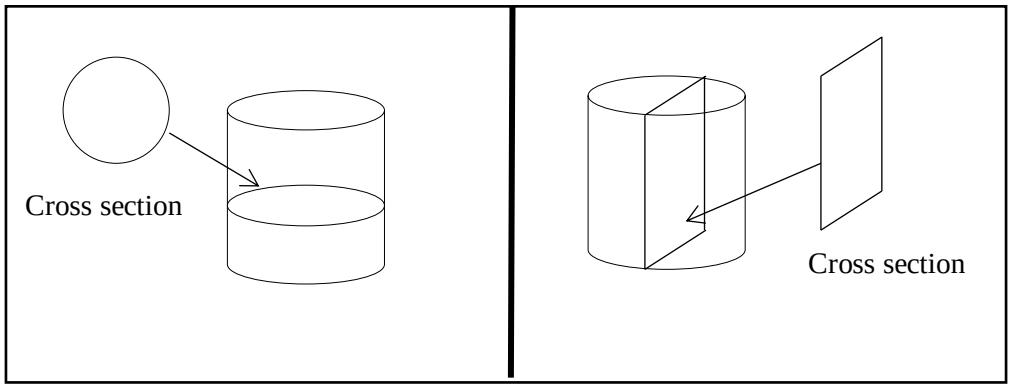

Figure 2.1 Cross Sections for Cylinder Shapes Objects

2.3 Stereo Vision

Computer stereo vision is the extraction of 3D information from digital images, such as obtained by a CCD camera. By comparing information about a scene from two vantage points, 3D information can be extracted by examination of the relative positions of objects in the two panels. This is similar to the biological process

Stereopsis: Stereoscopic images are often stored as MPO (Multi Picture Object) files. Recently, researchers pushed to develop methods aimed to reduce the storage needed for these files to maintain high quality of the stereo image.

In traditional stereo vision, two cameras, displaced horizontally from one another are used to obtain two differing views on a scene, in a manner similar to

human binocular vision. By comparing these two images, the relative depth information can be obtained in the form of a disparity map, which encodes the difference in horizontal coordinates of corresponding image points. The values in this disparity map are inversely proportional to the scene depth at the corresponding pixel location.

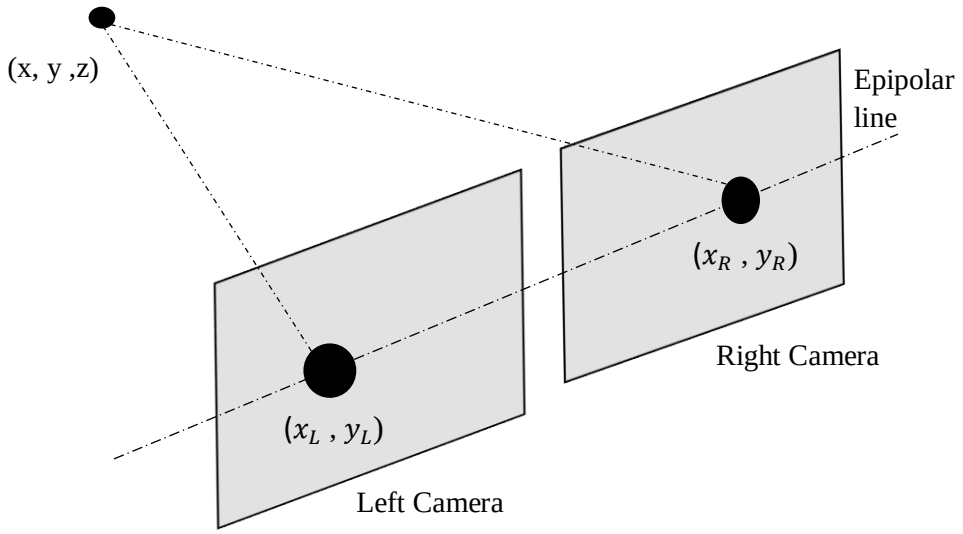

Figure 2.2 Structure of Stereo Vision

For a human to compare the two images, they must be superimposed in a stereoscopic device, with the image from the right camera being shown to the observer's right eye and from the left one to the left eye. The structure of stereo vision is shown in Figure 2.2.

In a computer vision system, several pre-processing steps are required.

1. The image must first be undistorted, such that barrel distortion and tangential distortion are removed. This ensures that the observed image matches the projection of an ideal pinhole camera.

2. The image must be projected back to a common plane to allow comparison of the image pairs, known as image rectification.

3. An information measure which compares the two images is minimized. This gives the best estimate of the position of features in the two images, and creates a disparity map.

4. Optionally, the received disparity map is projected into a 3D point cloud. By utilizing the cameras' projective parameters, the point cloud can be computed to get the surface information of objects so that it provides measurements at a known scale.

The active stereo vision is a form of stereo vision which actively employs a light such as a laser or a structured light to simplify the stereo matching problem. The opposed term is passive stereo vision. Conventional structured-light vision (SLV): The conventional structured-light vision (SLV) employs a structured light or laser, and finds projector-camera correspondences.

Conventional active stereo vision (ASV): The conventional active stereo vision (ASV) employs a structured light or laser, however, the stereo matching is performed only for camera-camera correspondences, in the same way as the passive stereo vision.

Structured-light stereo (SLS): There is a hybrid technique, which utilizes both camera-camera and projector-camera correspondences.

2.4 Structured Light Projection Method

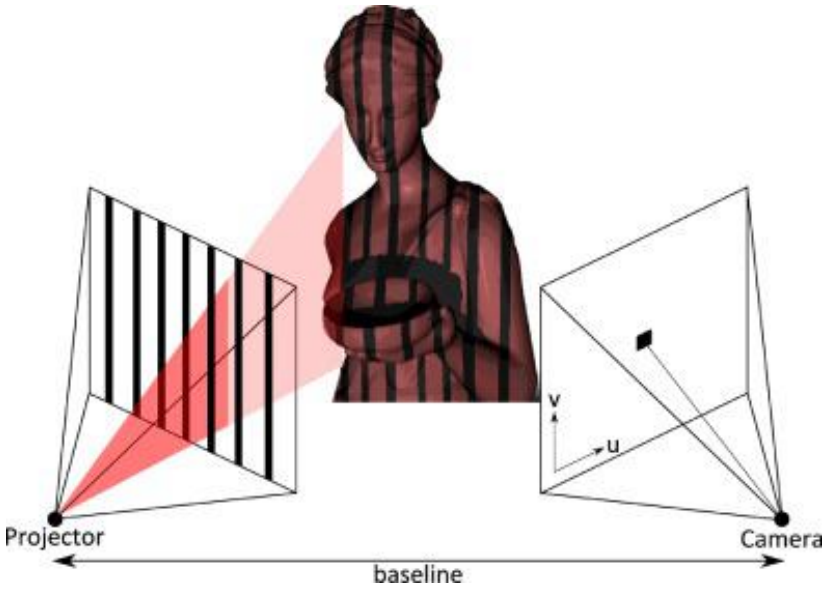

Figure 2.3 Principle of structured light based systems

Structured-light projects a pattern of light on the subject and looks at the deformation of the pattern on the subject. The principle of structured light based systems is shown in figure 2.3 [12]. The pattern is projected onto the subject using either an LCD projector or other stable light source. A camera, offset slightly from the pattern projector, looks at the shape of the pattern and calculates the distance of every point in the field of view.

Structured-light scanning is still a very active area of research with many research papers published each year. Perfect maps have also been proven useful as structured light patterns that solve the correspondence problem and allow for error detection and error correction.

The advantage of structured-light for 3D scanner is speed and precision. Instead of scanning one point at a time, structured light scanners scan multiple points or the entire field of view at once. Scanning an entire field of view in a fraction of a second reduces or eliminates the problem of distortion from motion.

There are three types for 3D reconstruction using structured-light projection method: from point clouds, from a set of 2D slices and from laser scanner.

2.5 Time of Flight

Time of flight is a property of an object, particle or acoustic, electromagnetic or other wave. It is the time that such an object needs to travel a distance through a medium. The measurement of this time (i.e. the time of flight) can be used for a time standard, as a way to measure velocity or path length through a given medium, or as a way to learn about the particle or medium. The traveling object may be detected directly or indirectly (e.g., light scattered from an object in laser Doppler velocity).

The principle operation of time of flight camera is shown in figure 2.4 [2]. Camera including time of flight is a range imaging camera system that resolves distance based on the known speed of light, measuring the time of flight of a light signal between the camera and the subject for each point of the image. It is a class of scanner less, in which the entire scene is captured with each laser or light pulse, as opposed to point-by-point with a laser beam such as in scanning systems.

The most used time of flight camera devices are direct time of flight imagers. These devices measure the direct time of flight required for a single laser pulse to leave the camera and reflect back onto the focal plane array. It is also known as “Trigger mode”, which are the 3D images captured using this methodology. The images complete spatial and temporal data and also record full 3D scenes with single laser pulse. This allows rapid acquisition and rapid real-time processing of scene information.

The application areas are used for automotive applications, human-machine interfaces and gaming, measurement and machine vision, robotics and earth topography.

There are various types of light sources for time of flight applications, the most common ones being infrared (IR) Light-emitting diode (LED) arrays and laser beams. Laser based applications such as Light Detection and Ranging (LIDAR) are more expensive and involve moving parts due to the fact that only one depth point can be acquired at a time, whereas the IR arrays are capable of capturing the entire FOV at once, providing depth images at a higher frame rate.

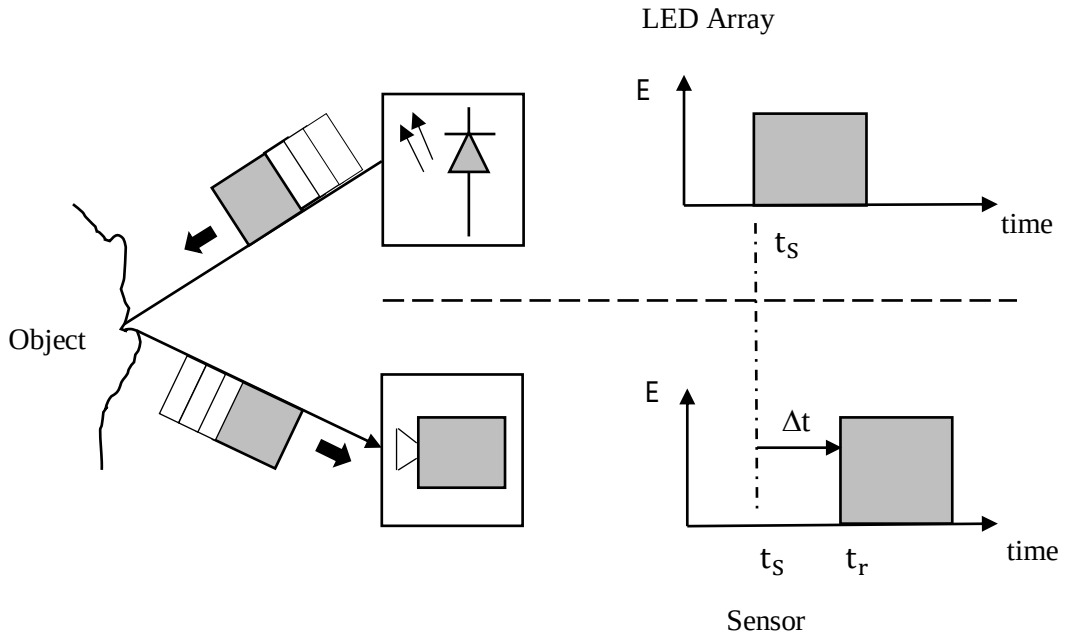

Figure 2.4 Principle operation mode of a time of fight camera

2.6 Goodness of Fit, Statistical Testing Model

The goodness of fit of a statistical model describes how well it fits a set of observations. Measures of goodness of fit typically summarize the discrepancy between observed values and the values expected under the model. In the analysis of variance, one of the components into which the variance is partitioned may be a lack-of-fit sum of squares.

There are two types of goodness of fit testing model, regression analysis and fit of distribution. Model fitting are used for evaluating the robustness, uniqueness, and sensitivity of parameters obtained from model of interest. A powerful tool is improved for data analysis and understanding the limitations on model parameters used for system characterization and distinguishing normal from abnormal populations.

For model fitting, goodness of fit measures for linear regression's attempts to understand how well a model fits a given set of data. Models almost never describe the process that generated a dataset exactly. The models approximate reality. However, even models that approximate reality can be used to draw useful inferences or to prediction future observations.

The steps to perform for model fitting are:

1. Finding the estimated primitives shapes by using curve or circle estimated functions.

2. Calculating the error fitting by subtracting the actual to corresponding estimated values.

2.7 Related Work

Currently, the least squares (LS) method has been most widely used in data fitting. The commonly used basis functions are polynomials, rational functions, Gaussian, exponential, smoothing spline in curve fitting, the B-spline, the non-uniform rational B-splines (NURBS), Bézier surfaces, and radial basis function in surface construction. Simultaneously, the deformations of LS as RLS (recursive least squares), TLS (total least squares), PLS (partial least squares), WLS (weighted least

squares), GLS (generalized least squares), and SLS (segmented least squares) have also been put forward. However, all the above LS based methods are global approximation schemes which are not suitable for large amount of data, irregular or scattered distribution cases. So the moving least squares (MLS) method which is local approximation was proposed in measurement data processing.

The MLS approximation was introduced by Lancaster and Salkauskas for surface generation problems [21]. It has been used for surface construction with unorganized point clouds, regression in learning theory, and sensitivity analysis. However, the major applications of MLS are to form a lot of meshless methods, as the diffuse element method (DEM), the well-known element-free Galerkin method (EFGM), and the meshless local Petrov-Galerkin method. These kinds of methods have high computational precision and stability. The disadvantage of the MLS lies in the algebra equations system that is sometimes ill-conditioned, so Cheng and Peng [26] proposed the improved method. The error estimates and stability of MLS and the variation as complex or Hermite [28] were intensively discussed. On the whole, the research processes of MLS approximation theory are much less than applications. Treated as simultaneous estimation of position and shape, point cloud fusion results in an errors-in-variables problem. Random Sampling Consensus (RANSAC) was utilized to estimate the parameters of cylinders and other simple geometric shapes.

A tracking approach for fitting linked cylindrical approximations to a human body is based on iterative methods such as Iterative Closest Point (ICP). From the viewpoint of point cloud reduction, relevant approaches are, Random Hypersurface Models (RHMs) [9] are a further method for extended object tracking, which allow for modeling complex extended objects.

CHAPTER 3

PRIMITIVE SHAPES FITTING USING 3D DATA

Nowadays, robotic technology is very popular in many research areas in order to explore in industrial applications, agriculture, graphing objects and scientific research areas. In recently years, three-dimensional measurements using RGB-D sensors has become popular in robot vision systems.

In the same case, RGB-D sensor is also used to get the point cloud data of objects. The easy access of RGB-D usage and its feasibility called to capture motion or modeling systems that do not require high accuracy. RGB-D sensor becomes very attractive because there is no limitation on the measurement area size since individual 3D point sets recorded from different positions can be combined on the computer.

3.1 RGB-D Sensor

A robot communicates the real world with sensors and actuators, and the information gathered by the sensors is then processed to obtain a desired result. Sensing ranges from obtaining black and white images of the surroundings of the robot to measuring electromagnetic waves or atmospheric parameters.

In solving the problem of getting image acquisition, the 3D sensor is the best to provide good quality in producing the acceptable results with noisy and highly distorted images, so the quality of the acquisition equipment is required. However, better equipment is often expensive and difficult to use and the recent development of affordable and open source devices has led the scientific community to search for a midway solution.

There are such devices like Microsoft Kinect [19], The Asus Xtion or the Intel RealSense provide the necessary tools for developing both affordable and reliable solutions. The figure of devices are shown in Figure 3.1.

Asus Xtion 2 Intel RealSense SR300 Kinect V2

Figure 3.1 RGB-D Sensors

3.1.1 KINECT Sensor

Microsoft KINECT sensor is a peripheral device that used to apply in Xbox 360, webcams, Microsoft windows PCs and many functions as shown in Figure 3.2. KINECT sensor includes camera for RGB images and also depth sensor for depth image as shown in Figure 3.3. The depth sensor in KINECT applies the time-of-flight technique. Therefore, it can get the depth map of objects which enters to the sensor. Then, all the pixels which can be seen KINECT measures distance from the sensor to the object using time of flight technique. This can solve a variety of computer vision problems. Actually, point cloud data are represented by verifying the angles from sensor to objects and the distance. The distance from the point in the point cloud to the object is depth values. A depth image stores the depth value of each pixel for various directions or rays. Therefore, the value stored at the pixel is the depth along the rays that go before hitting a point from the point cloud data.

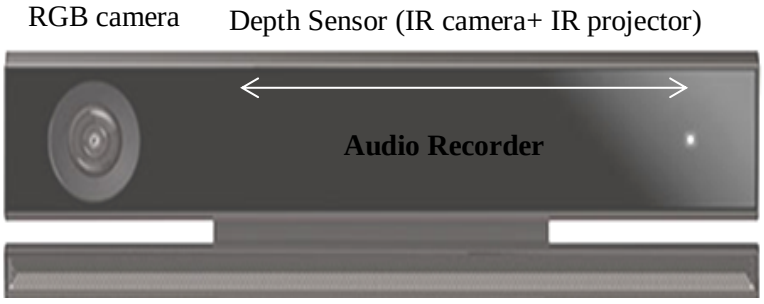

Figure 3.2 KINECT Sensor

Figure 3.3 KINECT Depth Image

3.1.2 Asus Xtion 2

RGB-D sensor (Asus Xtion II) is shown in Figure 3.4. It is used as a three-dimensional measurement instrument. Its depth sensor provides sharp and clear depth image. It can detect details of objects. The specification of Depth sensor is shown in table 3.1.

Table 3.1 Xtion 2 Specifications

Depth Image Size	640 x 480@30fps
RGB Resolution	2595 x 1944 @15fps (5MP)
Field of View	Depth: 74º H, 52º V,90º D RGB: 75.6º H,60º V, 87.9º D (Horizontal,Vertical,Diagonal)
Distance of Use	0.8m ~ 3.5m
Dimensions	11 x 3.5 x 3.5 cm (LxWxH)

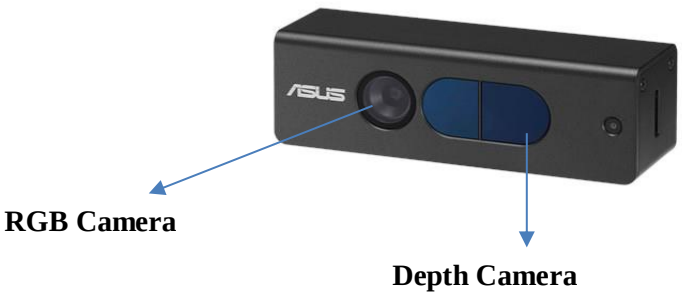

Figure 3.4 Asus Xtion 2

3.1.3 Intel RealSense

Intel has developed several versions of depth sensors based on its RealSense technology [14]. The Intel RealSense SR300 has a depth resolution of 640x480 at a nominal frame rate of 60 Hz and a FOV of 71.5 by 55 degrees. It also provides a 1920x1080 RGB image stream .The RealSense technology uses the coded or structured light technique for depth image acquisition, providing a depth range from 0.3 to 2 meters.

3.2 Measurement system of RGB-D Sensor

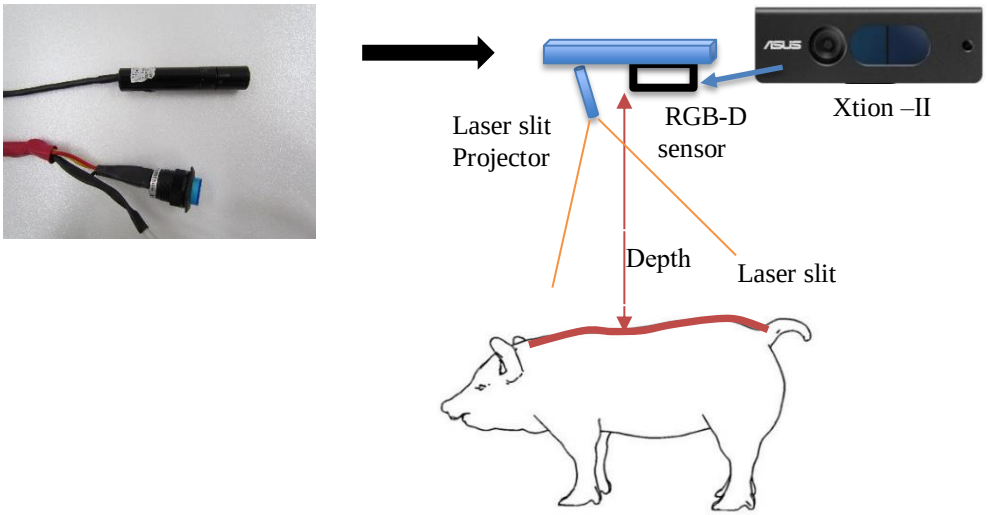

Figure 3.5 System Setup

The measurement system is shown in Figure. 3.5. The system is composed of a RGB-D sensor and a laser slit projector. Depth camera is used to convert the global coordinates through the pig model. The laser-slit projector is used to determine the direction of the measurement system against a pig.

RGB-D sensor (Asus Xtion II) is used as a three-dimensional measurement instrument. In implementation of measurement, taking a picture with the measurement target located at the center of Depth image and acquiring the luminance value which obtained the distance information of 16 bits at resolution of 640x480 pixels using ToF method. For capturing, the data is controlled by the switch as shown in Figure 3.6. The MAI - 2088 is a USB - connected IO board with 2 analog inputs, 8 digital inputs and 8 digital outputs. In addition to the IO control function, special API functions

have functions that can control external devices such as potentiometers, encoders, switches, and LEDs.

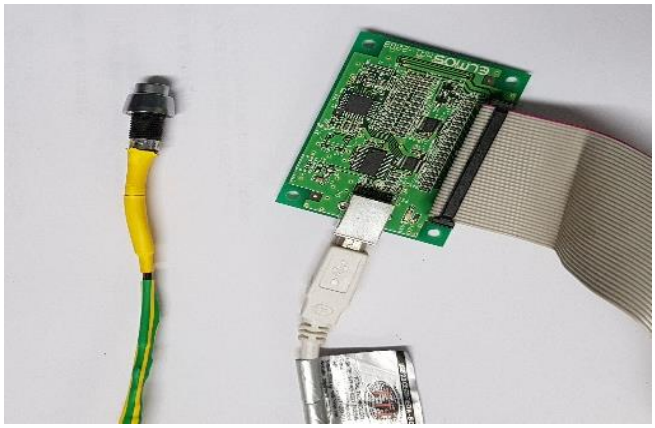

Figure 3.6 Switch for captured data

3.3 Getting Luminance Value of Measurement Target

In this study, a picture that is taken with the measurement target located at the center of the Depth image. By acquiring the luminance value at the center of depth image, it is possible to acquire the one of the luminance value on the measurement target.

The depth image obtained by sensor which includes the distance information (luminance value) of 16 bits at resolution of 640x480 pixels using ToF method. This ToF (Time of Flight) is one technique for measuring the distance to an object. This measures the distance from the flight time until the laser emitted from the light source is reflected by the target object and returned to the sensor. Besides the ToF method, there are methods such as a stereo camera and a structured light method. However, stereo cameras have low depth accuracy, disadvantages of poor performance in dark environments, structured lights are expensive and there is a disadvantage of poor performance in bright environments. However, ToF has the merit that it can be used without problems even in a dark environment and the depth accuracy is high. Median filtering is applied on removing noise in the image to get more actuate in procedure of object extraction. After extracting the measurement object, binary processing is performed with the threshold values in 10. The slope of measurement object is determined by the processing the binary operation in adjusting the movement of the object.

3.4 Setting range of measurement object

Depth based on the distance value at the center of image, set the range of the distance value to extract the measurement target from the depth image. In Figure. 3.7, the center position of the Depth image is indicated by a square, and this center position is located in the one portion of the pig body. Figure 3.8 shows the depth image of the measurement target. The principle of the range setting of the measurement object is shown in Figure 3.9. It gets the point and the distance value Z [mm] to Xtion II and sets the range according to the size of the measurement target. Volume shape in the range of -100 mm to +300 mm from the distance value at the center of the Depth image are stored. Thereby, even if there is another object near the measurement object, the volume only for the measurement object can be extracted.

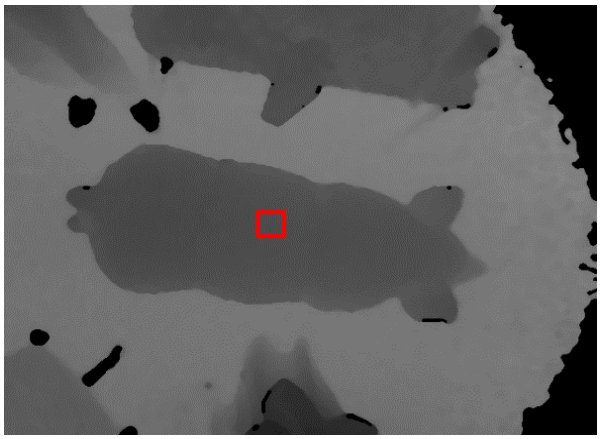

Figure 3.7 Center of measurement target

Figure 3.8 Depth Image from Xtion sensor

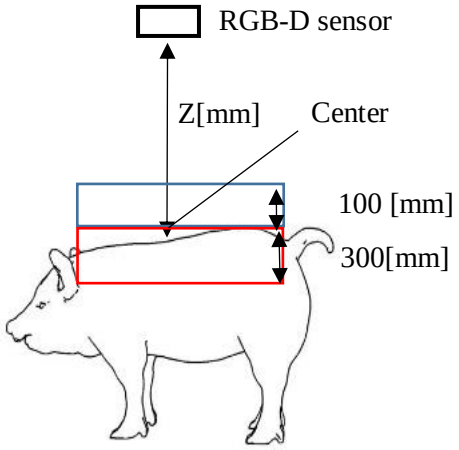

Figure 3.9 Setting range of measurement object

3.5 Noise Detection using Median Filter

Smoothing or image blurring is the simplest and more frequently used image preprocessing operation. There are many reasons for image blurring: to remove the noise, to sharpen contrast, to highlight contours and to detect edges. Therefore, image filtering is applied for smoothing operation. The most frequently used image filtering method is **Median Filter**. Image filters can be divided into linear or nonlinear filtering. Linear filtering is known as convolution filters as they are represented using matrix multiplication. Thresholding and image equalization are examples of nonlinear operation, median filter. Median filter is a nonlinear method, which is used to reduce the noises from digital images. Especially, it is very useful for removing salt and pepper type of noises.

The median filter works by moving through the digital images by pixel by pixel and replace each pixel value with median value of its neighborhood pixels. The patterns of its neighbor size is called window, which divides from the whole entire image using kernel size. The median is considered by sorting all the pixel values from the pixel values of window and replace that median pixel value to the selected pixel value. By using this procedure, it works to all pixels in images. When it has been completed all pixels, the noises are also reduced by median filter techniques. The depth image has a lot noise error from the sensor. It is impossible to see the original depth image data from sensor because of the noises in image detection. Median filtering is the best filtering technique in detecting the noise removing salt and pepper

type of noises. The result of original image and filtered image using median filter are shown in Figure 3.10.

Original Image Filtered Image

Figure 3.10 Median Filter

3.6 Extraction of Measurement Object

The object extraction is shown in Figure 3.11. Pig shape data can be extracted using ellipse-fitting algorithm. In the pig farms, all pigs may be connected each other. It causes the difficulties in measurement of pig weight in such case. Therefore, the object recognition can be helpful for detection of pigs in extraction process. The area of pig that occupied in ellipse is calculated. Green line curve is used for object in center position or not. If the object is in center, the line curve is shown like in Figure 3.11 by applying RANSAC algorithm. Line graph is applied to observe the measurement object in depth image. The green color is represented the measurement object on the computer.

RANSAC is the abbreviation of Random Sample Consensus. It is a general algorithm that can be used with other parameter estimation methods in order to obtain robust models with a certain probability when the noise in the data doesn't obey the general noise assumption. It is selected randomly the minimum number of points required to determine the model parameters.

Binary processing of depth image is performed after extracting the measurement object. The binalization process is a process of converting an image signal represented by black and white. A threshold value is determined in each pixel that if it is exceeding the threshold value, it is changed white and lower than the exceed values, it represented as black. In this system, binarization was performed with

threshold value 10. Figure. 3.12 shows the result of the binarization process. The rotation of object in horizontally as shown in Figure 3.13. There are many things in measurement area. So, the object cannot be extracted clearly. If the object is not horizontal, the measure of length and circle cannot be accurate. The measurement object has an inclination, the circle or length measuring. Therefore, if the angle of object increased more and more, the error may occur.

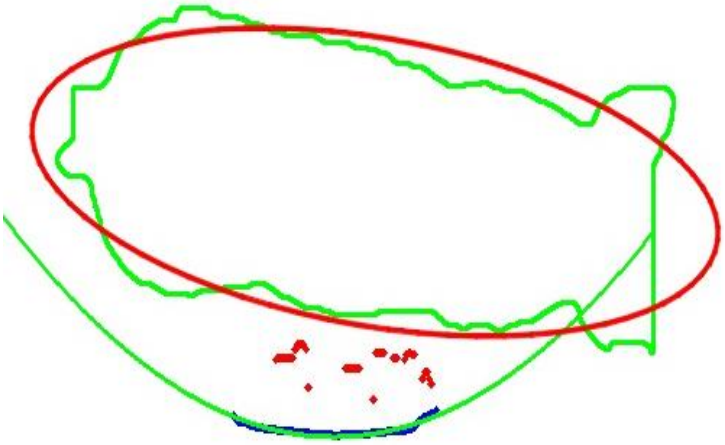

Figure 3.11 Extraction of measurement object using graph of line curve

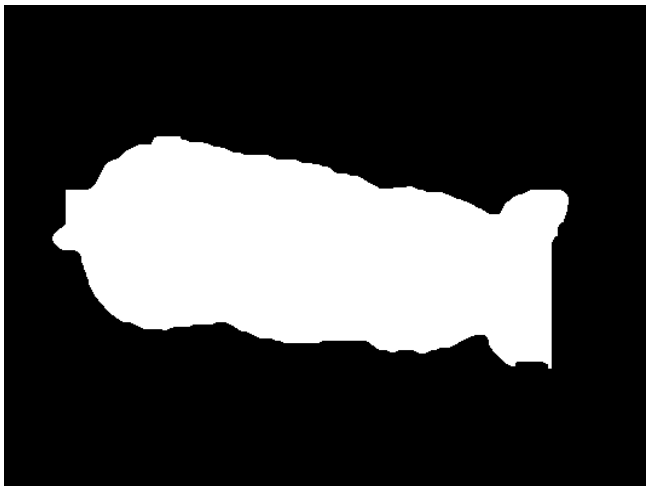

Figure 3.12 Binarization

3.7 Acquisition of 3D data

The distance from camera to object obtained the depth information is used in extraction of measurement object. The three-dimensional data can be measured by the principle of (*Y, Z*) plane. Xtion depth sensor is based on ToF method. The luminance

value on the object is nearly the same as it is located on the surface of the same object. Therefore, the distance value Z [mm] between the depth sensor and the target object can be used for the extraction process.

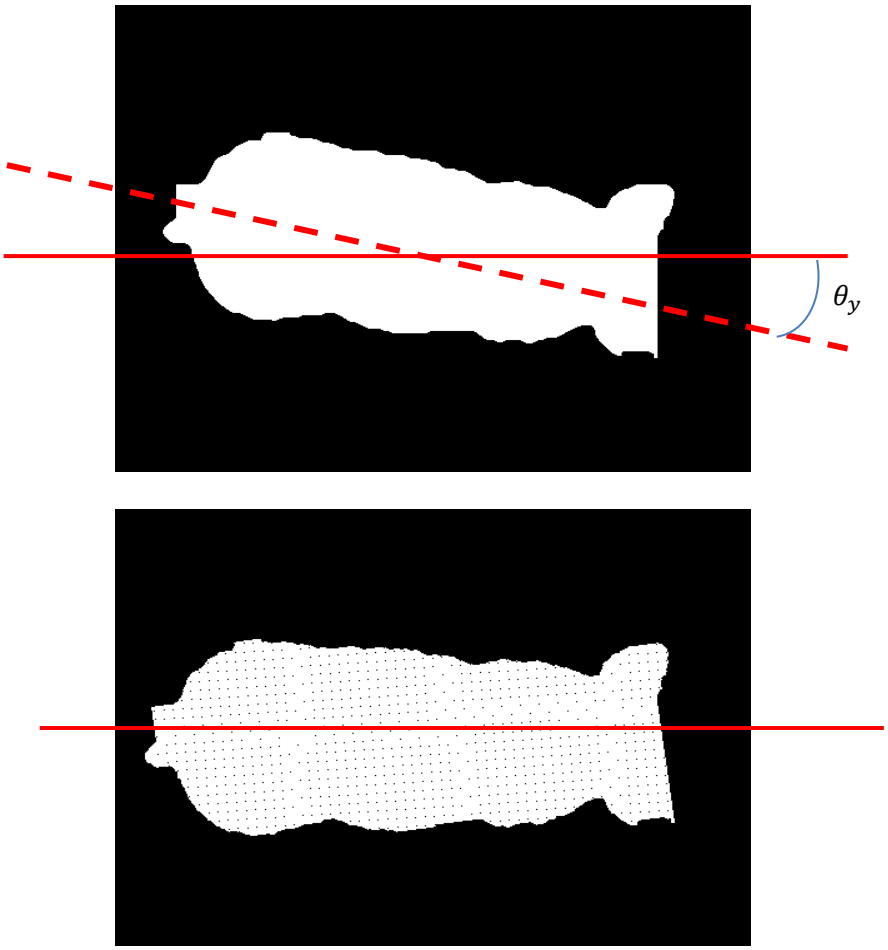

Figure 3.13 Result of rotation object

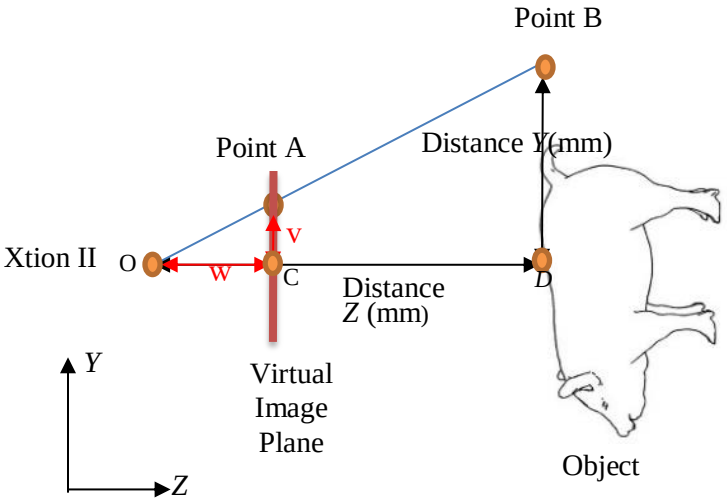

Figure 3.14 Principle of obtaining Y coordinate

Expressions for obtaining the remaining three-dimensional data (*X*, *Y*) coordinates from this *Z* value are shown in equation (3.1) and equation (3.2). The point (*u*, *v*) of these equations shows the coordinates in the Depth image, and *w* is the distance between the light source and the virtual image plane. Equation (3.1) is obtained because of the similarity relationship between triangle AOC and triangle BOD in Figure 3.14, and equation (3.2) is obtained from the same principle in the (*X*, *Z*) plane.

$$Y = -\frac{z}{w}\, v \tag{3.1}$$

$$X = -\frac{z}{w}\, u \tag{3.2}$$

Figure 3.15 shows the (X, Y) plane in the virtual image plane. The virtual image plane is the theoretical image when photographing the measurement object with Xtion. However, the number of pixels and the depth image actually acquired are the same, and since the Depth image is 640 × 480 pixels, the virtual image plane is also 640 × 480 pixels. Equation (3.3) is obtained when the y coordinate from the upper left of the virtual image plane to the point B is y1, and when it is combined with the equation (3.2), therefore the equation (3.4) is obtained. With the same principle, it is also possible to change to the equation (3.5) on the X coordinate.

$$v = 240 - y1 \tag{3.3}$$

$$Y = -\frac{z}{w}\,(240 - y1) \tag{3.4}$$

$$X = -\frac{z}{w}(320 - x1) \tag{3.5}$$

Using these equations, the three-dimensional point cloud data with top and side views is shown in Figure 3.16. This point cloud data is extracted by applying the region growing method in ellipse fitting algorithm. Three-dimensional data is acquired only on the measurement target object. Camera detects with object positioned at the center of Depth image. After getting the luminance value at the center of the Depth image, it is possible to obtain one portion of pig in capturing. Thereby, even if there is another object in the vicinity of the measurement object, the distance value only for the measurement object can be acquired.

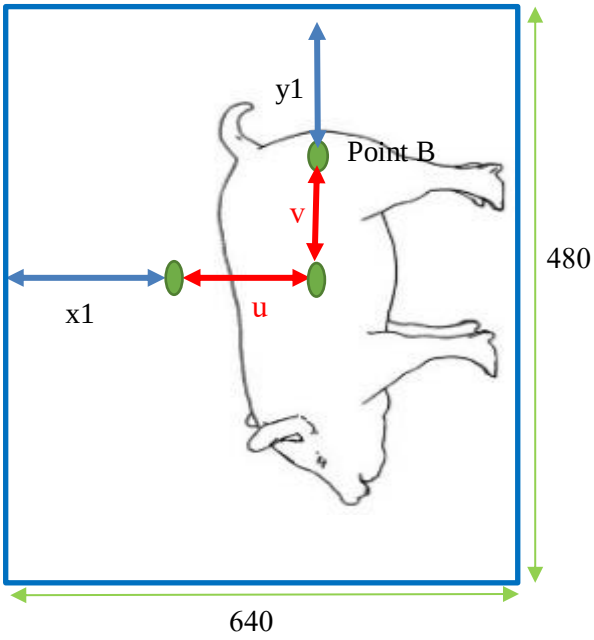

Figure 3.15 (X Y) Virtual Image Plane

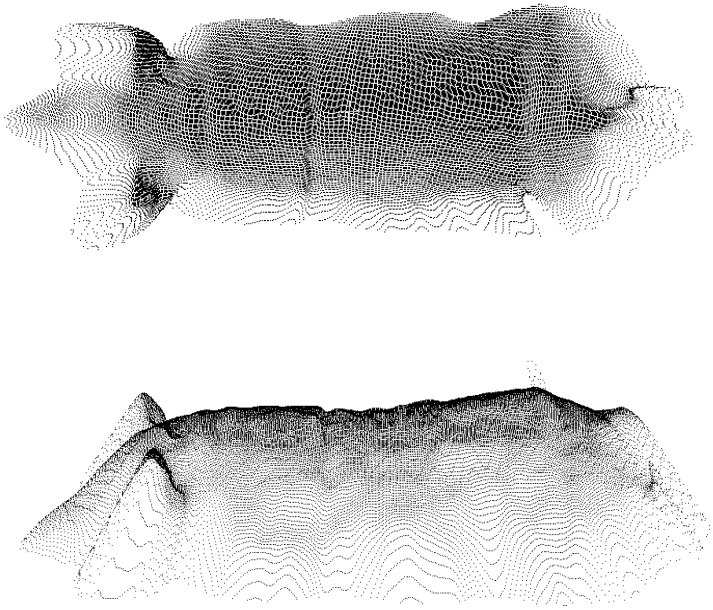

Figure. 3.16 Three-dimensional data of top and side view

3.8 Splitting 3D Data

In the obtained three-dimensional data, data is divided and stored with a section perpendicular to the x-axis direction. In splitting data, each section is

separated by 30 mm apart, and the x coordinate in one section is preserved with a width of plus or minus 3 mm. Segmentation of the section of pig is more convenient to measure the body length and girth in estimation process.

Figure. 3.17 shows the result of the splitting data dividied by 30 mm. If the cross-section value is larger, the detection of body length is larger. If the length is small in processing of body length, the cross section becomes smaller than 30 mm. But there are a few errors, so the measurement of pig cannot get the accurate data. Therefore, the pig is reconstructed in the computer by arranging all of cross-sections along with X-axis.

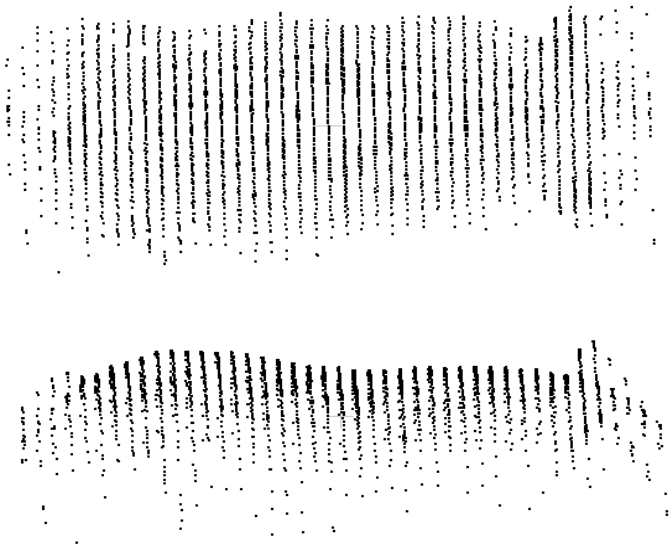

Figure. 3.17 Cross sectional data divided by 30 mm

3.9 Detection of Body Length

In estimation of body length, the length can be estimated from the obtained data using model curve fitting techniques. The least square fitting result is the most accurate fitting result with the less error rates. The length along the spine is measured through ear-to-tail position to estimate the weight of pig. The length of the model pig is shown in Figure 3.18.

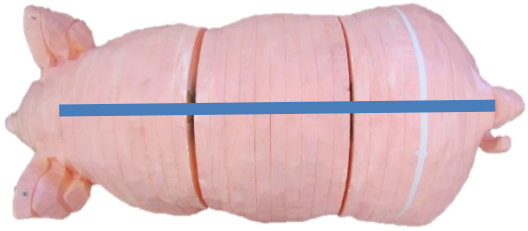

Figure. 3.18 Length measurement of pig model

In the detection of pig head, the top position can be observed in each cross section by using two power curve model fitting. All of the top position points are almost in the middle of cross sections, and the backbone area of pig is shown in Figure 3.19. However, some of the top positions are missed from the center of cross sections which cause by ears position of pig. It cannot well be detected the top positions in the case of cross sections with ears. The top positons become biased to ear positons on measurement of pig body. Therefore, the detection of body pig length will apply this consideration to remove the pig head for the measurement process.

For the detection of tail position, the template matching is applied in matching tail of pig from binary image. The procedure of detecting tail is shown in Figure 3.20. Template matching technique compares the same portions of images against to another image. It can be used in classifying objects in the image. This template matching is usually used in binary level image. Even the small matching process, it can detect accurately the matching process. The process of matching is based on a pixel-by-pixel basis. It also needs the template image and looks in source image to perform the matching process.

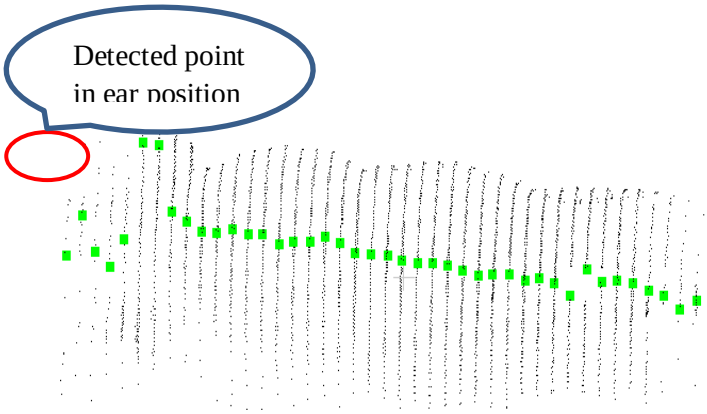

Figure 3.19 Top position of pig in each cross section

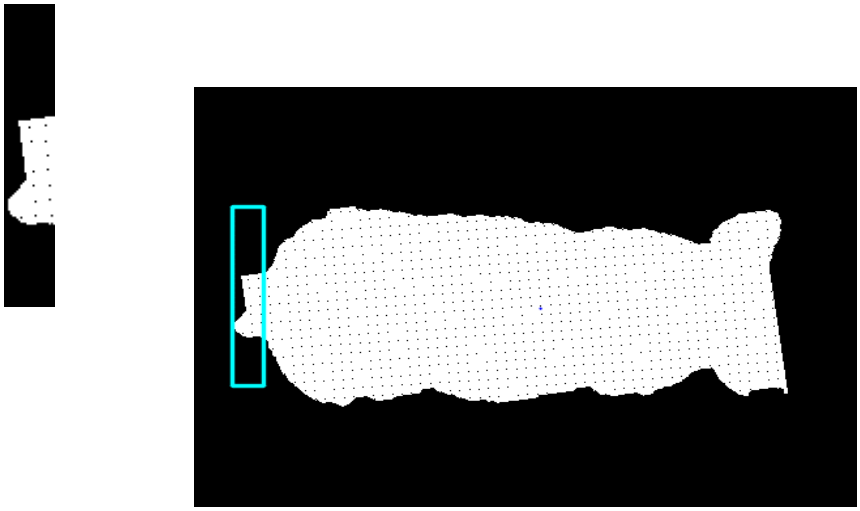

Figure 3.20 Detection of pig tail using template matching

The length of pig can be estimated from the obtained 3D data after getting the detection of pig head and tail position. In the case of finding the length of pig, Euclidean distance equation (3.6) can be used in process.

$$d = \sqrt{(x_2 - x_1)^2 + (y_2 - y_1)^2 + (z_2 - z_1)^2} \tag{3.6}$$

3.10 Primitive Models Estimation

All the computer aided systems can provide the users with the primitive shapes entities, which can be classified into Analytic and Synthetic entities. Analytic entities are points, lines, arcs, circles, fillets, chamfers and conic sections. Synthetic entities are cubic spline, B spline and Bezier curves. Mathematically, all of these synthetic entities can be represented by construction smooth data fitting that passes through given data points. Data fitting is a type of regression analysis, which is used to find the best fit primitive shapes using a series of data points.

The data point is estimated to represent the shape of some unknown planar shape. The final curve is called target curve or target shape. Therefore, it is very important to receive the automatic shape generation, which can set the point to target shape. Laser light structured light projection gains more and more importance in last few years ago. Large sets of 3 dimensional point data can be got by using time of flight method and Xtion II. All of these data can be used to get the efficient and effective organization of data points to primitive shapes.

3.10.1 Least Square Curve Estimation

Least Squares is a method of curve fitting that has been popular for a long time. It minimizes the square of the error between the original data and the values predicted by the equation.

In the case of curve fitting, it is very important to consider which types of curve fitting should be used for curve fitting from input data points. There are linear, polynomial, exponential, and logarithmic and power approaches to use for curve fitting.

3.10.1.1 Linear Curve Estimation

Linear curve fits a straight line through the input data points using equation (3.7). There is no data restriction which is associated with the curve fitting.

$$y = m_0 + m_1 * x \tag{3.7}$$

where m_0, m_1 are homogeneous parameters for polynomial curve.

3.10.1.2 Polynomial Curve Estimation

Polynomial curve fits a curve through the input data points using equation (3.8). The more complex the curvature of the result, the higher polynomial order is required to fit the curve. There is no data restriction which is associated with this curve fit.

$$y = m_0 + m_1 * x + m_2 * x^2 + m_3 * x^3 + \cdots + mn * x^n \tag{3.8}$$

where m_0,…, mn are homogeneous parameters for polynomial curve.

According to the input data, this polynomial curve estimation is used to observe the curve of the best fit. However, this polynomial curve estimation can only be applied for 2 dimensional estimation of curve equation (3.9).

$$\begin{bmatrix} y_1 * y_1 & y_1 & 1 \\ y_2 * y_2 & y_2 & 1 \\ y_3 * y_3 & y_3 & 1 \\ & \vdots & \\ y_n * y_n & y_n & 1 \end{bmatrix} \begin{bmatrix} a \\ b \\ c \end{bmatrix} = \begin{bmatrix} z_1 \\ z_2 \\ z_3 \\ \vdots \\ z_n \end{bmatrix} \tag{3.9}$$

where $y_1 \dots y_n$ is the y-coordinates of data points, $z_1 \dots z_n$ is the z-coordinates of data points. *a,b,c* are the homogeneous parameters for estimation of polynomial curve.

3.10.2 Circle Estimation

The data points $\{(y_i, z_i)\}$ consider on the circumference of unknown circle's center and radius. In this case, there is unknown value for center and radius. Therefore, the average radius would be the average distance from each point to center. Actually, it can suspect that the desire center must be near the center of mass of the data points to construct the circle. But if all the points are evenly distributed around the circle, equation (3.10) comes up to measure the error between the estimated circle and data points.

$$(y-a)^2 + (z-b)^2 \tag{3.10}$$

where *y* is the y coordinate of data points, *z* is z coordinate of data points, *a,b* are the homogeneous parameters for estimation of the circle, r is the radius.

Circle from plain section, equation (3.11) is changed for data points:

$$y^2 + z^2 + Ay + Bz + C = 0 \tag{3.11}$$

where A,B,C are the homogeneous parameters for estimation of circle, y is the y coordinates of data points and z is the z coordinates of data points. By changing two dimensional circle equation (3.12) , the homogeneous parameters are obtained.

$$\begin{bmatrix} y_1 & z_1 & 1 \\ y_2 & z_2 & 1 \\ y_3 & z_3 & 1 \\ & \vdots & \\ y_n & z_n & 1 \end{bmatrix} \begin{bmatrix} A \\ B \\ C \end{bmatrix} = \begin{bmatrix} -y_1^2 - z_1^2 \\ -y_2^2 - z_2^2 \\ -y_3^2 - z_3^2 \\ \vdots \\ -y_n^2 - z_n^2 \end{bmatrix} \tag{3.12}$$

By using all these parameters, the center coordinates of circle, radius of the circle values will be resulted out with following equations (3.13) , (3.14) and (3.15).

$$y_c = -A/2 \tag{3.13}$$

$$z_c = -B/2 \tag{3.14}$$

$$r = \sqrt{(y_c^2 + z_c^2) - C} \tag{3.15}$$

where y_c is the center coordinates of y, z_c is the center coordinates of z and r is the radius. The following equation (3.16) is used to observe the point on the circle circumference

$$P' = C + \left(\frac{P-C}{|P-C|}\right) * R \tag{3.16}$$

where *C* is center, *P* is external point, *R* is radius.

In approximation of circle of pig, one section of circle in separating three-dimensional data is shown in Figure 3.21. The distance between the center coordinates (a, b) of approximate circle and the point on one cross section of three-dimensional data is r. The circle is officially modeled from the calculated equation of the circle, and the result of approximation the whole portion of pig is shown in Figure 3.22. The coordinate of each point of the circle are expressed by equation 3.17. The range of θ is 0 to 2π, and the angle is acquired and saved with an inclination of 3 degrees each.

$$\left.\begin{aligned} x &: 30\ mm \\ y &= a + r \times cos(\theta) \\ z &= b + r \times sin(\theta) \end{aligned}\right\} \tag{3.17}$$

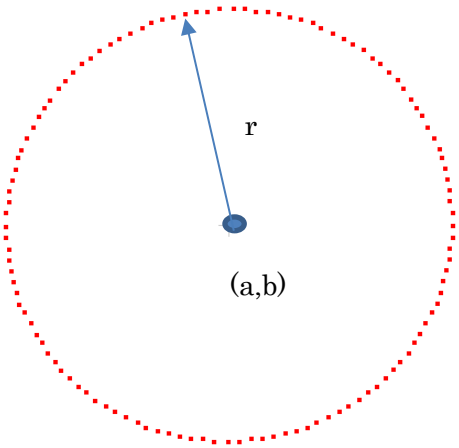

Figure 3.21 One section of circle approximation in 3D data

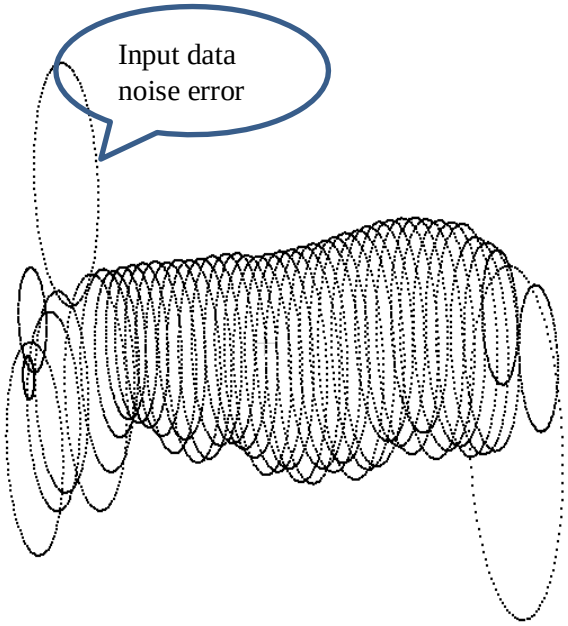

Figure 3.22 Approximation of circle in pig model

In the detection of girth position, it is calculated using approximated circle at each cross section. The circumference is estimated by the data position of chest. To find the girth, template matching can get the position of chest accurately from the given image. It is a high-level machine vision method which determines the components of a figure which matches a predefined template. This technique is repeated in the whole images to find the best match whatever the shape in the image. Using template matching, it is required two crucial segments.

(1) Source Image which is an original image to find out a match to template image.
(2) Template Image which a patch image to be compared to the source image and discovers the best matching region.

Using this technique, the girth position can be found easily. The detection of chest position using template matching is shown in Figure. 3.23.

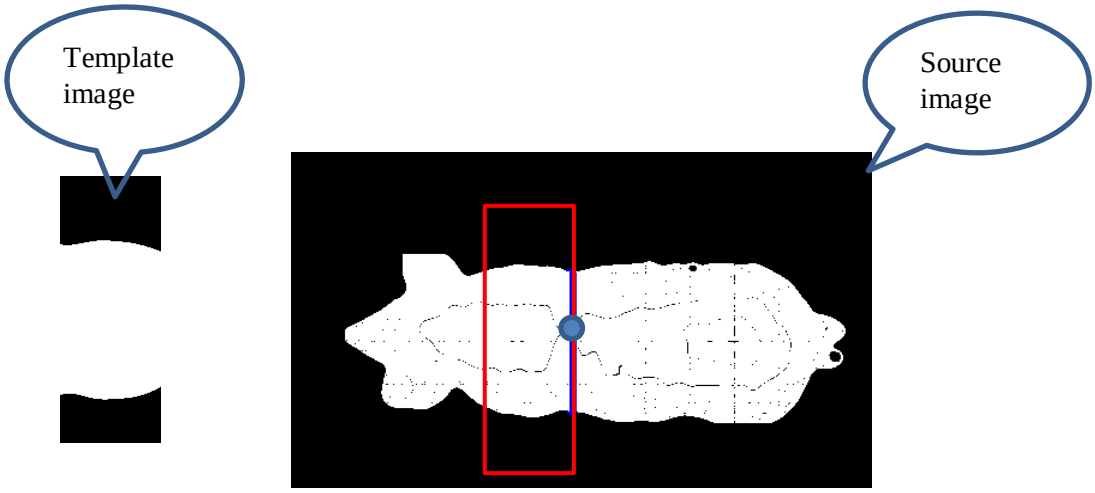

Figure 3.23 Detection of chest position in binary using template matching

After getting the chest, the position value is converted the three-dimensional data and make the circumference in the closest point of point cloud data. Let the length of the circumference of the object to be measured be L, and obtain it from equation (3.18). In this measurement system, the circumference is obtained for each cross section modeled on the circle, and the average value is taken as the diameter of the measurement object. When obtaining the average value, the cross section at both ends of modeling the circle is excluded. This is because there may be outliers. In the point cloud modeling of the circle to be measured, comparison was made between the case of obtaining the diameter from the sum of the distances between the two points and the case of obtaining the diameter from the equation (3.18).

$$L = 2\pi r \tag{3.18}$$

3.11 Adjusted R-square Regression Model

In case of error fitting, it is not guarantee that both of the two variables are exactly same by using only their parameters values. Actually, there is no guarantee to be the best fit with the estimated shapes with the input data points that are to be the same approximately. To perform adjusted r-square regression model, the following two steps are needed:

1. Finding the estimated primitives shapes by using curve or circle estimated functions.

2. Calculating the error fitting by subtracting the actual values to corresponding estimated values.

Adjusted R-square (R^2_{adj}) regression model is a modified version of R-squared that has been adjusted for the number of predictors in the model. This adjusted R-squared increases only if the new term improves the model more than would be expected by chance. It decreases when a predictor improves the model by less than expected by chance. The adjusted r-squared uses goodness of fit, statistical analysis, which is used to consider how much one variable differs from second variable. This adjusted r-square gives the percentage variation in one variable to second variables. R^2_{adj} is mostly similar to the correlation coefficient. Therefore, it can give the linear relationship information how strong relationship between the two variables. R can be considered as the percentage. It can give a result of how much point cloud data can fall within the estimated shapes upon using this regression equation. The higher the percentage values from regression equation, the higher the relationship between original data points and estimated model. The coefficient of determination can also be negative. When that value goes to negative, it means that the original data is bad fit to the estimated model.

To find the adjusted r-square coefficient of determination: it is easier to calculate the coefficient of determination of r^2 equation (3.19)

$$r^2=\frac{ssot-sse}{ssot} \tag{3.19}$$

where r=r-square coefficient of determinations, sot (total sum of square) means $\sum (X_i\text{-}mean)^2$ that measure the variation of the observed values around the mean and sse (Error sum of square) mean $\sum (X_i\text{-}error)^2$ that measure the variation of the observed values and regression line. , X_i=observed data points and mean is the mean of observed data points and error is the variation of each point from observed data points.

To find the adjusted coefficient of determination ($\bar{R}^2$): it is closely related to the coefficient of determination (also known as r^2) which shows the proportion of variation explained by the estimated regression equation (3.20).

$$\bar{R}^2 = 1 - \frac{(1-R^2)(N-1)}{N-p-1} \quad (3.20)$$

where R^2 is sample R-square , p is the number of predictors which are independent variables and N is the number of observations.

For a good regression model, the testing variables that effect the response in order to avoid biased results is important in regression model. The best model can be only as good as the variables in the analysis cannot be biased in progressing. One major difference between R-squared and the adjusted R-squared is that it accepted if all independent variables in the model affect the dependent variable. Adjusted R-squared that explained by only those independent variables that in reality affect the dependent variable. Therefore, the adjusted R-squared is the best to estimate the shapes of point cloud data correctly.

In this system, point cloud data of Xtion 2 3D sensor is used to estimate the curve and circle. This estimated values go to goodness of fit by using adjusted R-square regression model.

CHAPTER 4

DESIGN AND IMPLEMENTATION

The purpose of the system is to analyze the precision results of RGB-D sensor for model fitting and compare the result of length and circle with the model data of pig. In this chapter, the system flow diagram and implementation of the system are described in detail. The evaluation and experimental results are also shown in this chapter.

4.1 System Flow Diagram of Proposed System

The overall system flow diagram for proposed system is shown in Figure 4.1. Users have to choose what they want to perform, three-dimensional point cloud data from RGB-D sensor. Firstly, the 3 dimensional point cloud data from RGB-D depth sensors enters in to this system. When it enters into this system, all of these data are separated with the line number to perform length and circle in measurement of pig. In the case of length and circle, users has two choices in each. In length measurement, there are two measurements such as length estimation and curve model fitting which is to analyze the correlation analysis of adjusted r-squared regression model. In the case of circle measurement, there are also two measurements such as circle estimation and circle curve fitting which is to analyze the correlation analysis of adjusted r-squared regression model. If the users chooses length estimation, the data is performed to estimate the length with ear-to-tail position and show the value of pig length. If the user chooses the curve fitting model, the data is measured the length of pig and calculating the correlation results of curve fitting which the model can be performed on the curve estimation and the estimated curve result is out. If user chooses the circle estimation, the data is performed the approximation circle of pig portion using ransac algorithm and find the chest position using template matching technique. If users chooses the circle model fitting, the data is made the circle of pig portion and the estimated curve circle and result of chest positons by applying adjusted r-squared regression model and output the result. Finally, it calculate the relationship between estimated curve and real point cloud data by using adjusted r-square regression model and output the results.

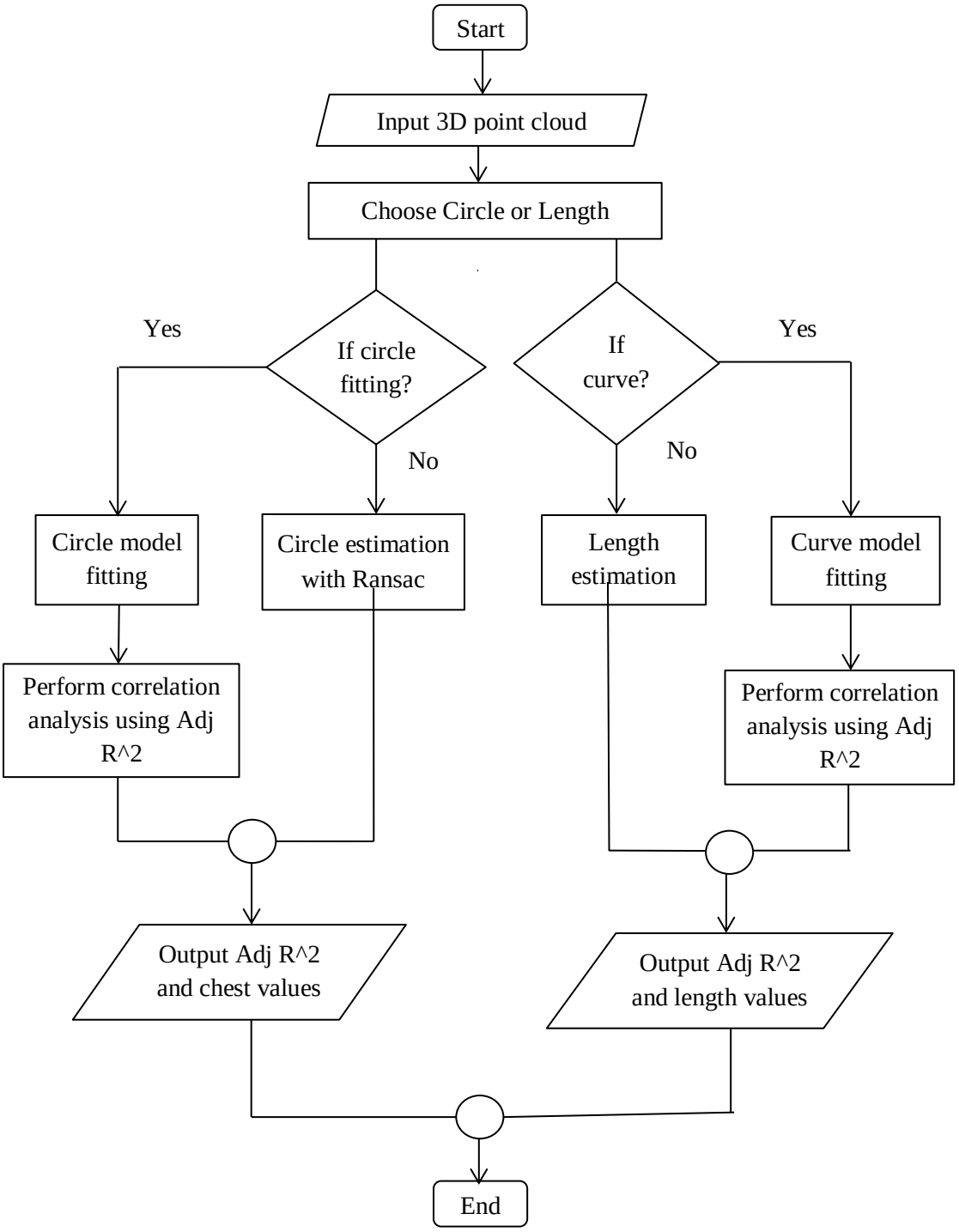

Figure 4.1 Overall System Flow Diagram for proposed system

4.2 Background Extraction of Measurement Object

In the case of background extraction, Figure 4.2 is applied by median filter. Actually, depth sensor is very sensitive to noise presence. Therefore, the presence of

more noise in sensor goes to the lower accuracy. It is very important to perform background extraction in order to obtain the more perfect point cloud data.

Firstly, the background image of the measurement area is captured. Generally, extraction of target can be executed by just taking the difference between background image and measurement image, but the slight changes of the external appearance generates noise and prevent the extraction process. In order to reduce the influence of external appearance, median filter is applied to the background image and measurement image. After that, image arithmetic operation is applied to median filter image. It is changed to binary image. Finally, moving object is extracted by executing "AND" operation between measurement image and extracted binary image as shown in Figure 4.3.

In the detection of angled process in extracting measurement target, it may occur some error due to the measurement area. There have a lot of objects in measurement area such as same other objects, the wall and so on. Therefore, the measurement object cannot be extracted clearly and accurately. If the measurement target is not horizontal, the point cloud data can't be perfect. In all the pig farms, all pigs may be connected each other. It caused the difficulties in measurement of pig in such case. The measurement target has an angle in each measurement, the point cloud examining is not perfect extraction. Therefore, if the angle of object become increased more and more, the error may be occur.

4.2.1 3-Dimensional Image Reconstruction from RGB-D Sensor

Figure 4.4 shows the 3 dimensional point cloud data of side view which is captured from depth sensor. Figure 4.5 shows the 3 dimensional point cloud data of top view which is captured from depth sensor. In Xtion 2 depth image, it has 640*480 resolution. The acceptable distance from depth sensor to object is from 500 mm (millimeters) to 3500 mm (millimeters). For depth map is 500mm, the acceptable black color is 7821 and white color is 65535. It has only 2 bits color codes for depth image. The three-dimensional data is obtained by capturing the center of measurement target. Camera detects the objects at the center position of depth image. Therefore, it is possible to get the whole portion of object in capturing process. Moreover, even if

another object in adjacency of measurement object, three-dimensional point cloud data of measurement object can be obtained.

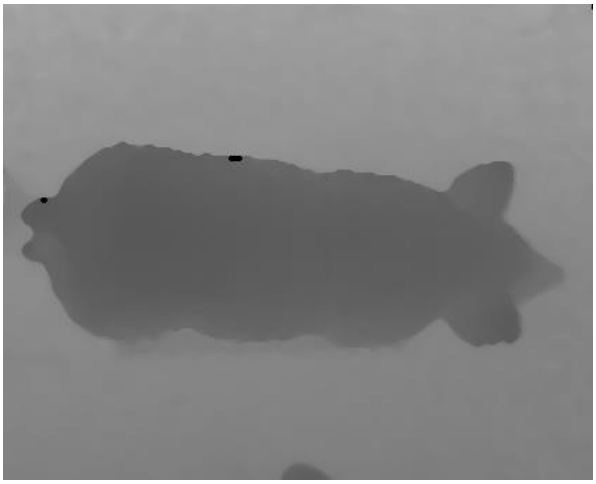

Figure 4.2 Background Extraction

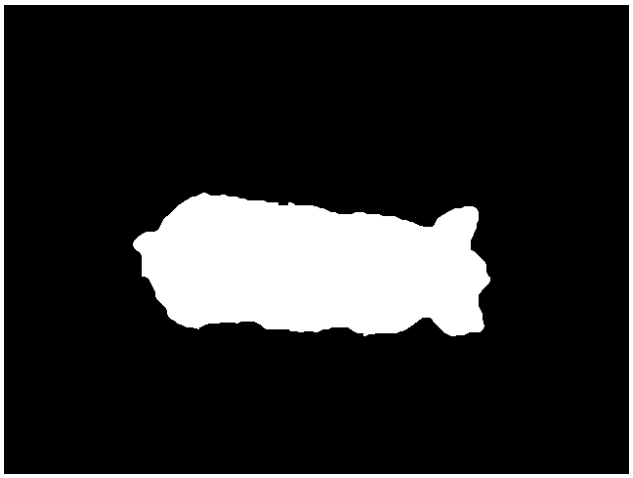

Figure 4.3 Binary Image

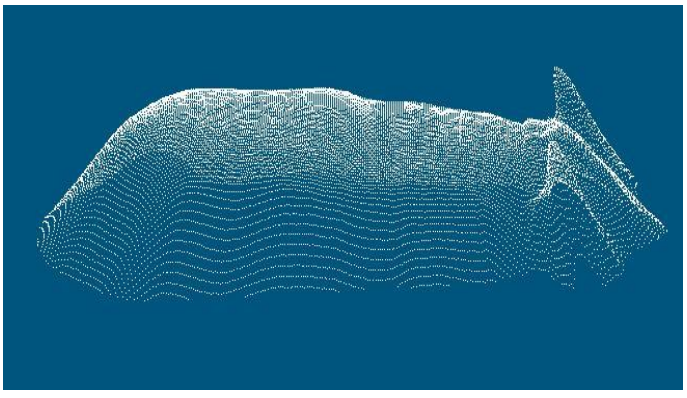

Figure 4.4 Side view of measurement object from Xtion II sensor

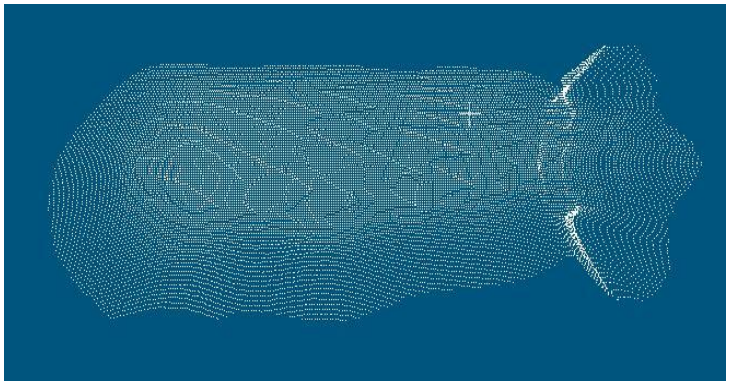

Figure 4.5 Top view of measurement object from Xtion II sensor

4.3 Curve Estimation

The data is split 30mm cross sections in each for RGB-D sensor. For curve estimation, linear regression model is used. In this case, this system only wants to know how well the system can verify the shapes of each cross section. For the curve estimation, the polynomial equation is applied to estimate the three-dimensional data shape. Therefore, x-coordinates are reduced in accord with the requirements of system.

In the obtained three-dimensional data, the data is divided and stored with a section perpendicular to the x-axis direction. Algorithm for curve estimation is shown in Figure 4.6. For 30 intervals cross sections, the curve model estimation using adjusted r-square regression model for sensor are performed.

4.4 Circle Estimation

There are 30 slits intervals of cross-sections for sensor. For circle estimation, circle geometry is used. In this case, this system only wants to know how well the system can verify the shapes of each cross section. Therefore, x-coordinates are with the requirements of system.

In circle estimation, the y coordinate and z coordinate consider how strong relationship in estimated circle with circle cross section.

For 30 slits intervals of cross-sections, the circle model estimation using adjusted r-square regression model for sensor are performed in circle estimation. Algorithm for circle estimation is shown in Figure 4.7.

Algorithm: Algorithm for curve estimation

Input: 3D data in order to perform circle model estimation

Output: R-square regression values for all slits lines

```
Begin
For j=0 -> size of cross section do
Begin
  Initialize x-coordinates with input data x coordinates
  Initialize y-coordinates with input data y coordinates
  Initialize z-coordinates with input data z coordinates
  Initialize size <- size of input data
  for i=0 -> size do
        Begin
          Initialize matrixA and matrixB
          martixA <- new matrix size of (size,3)
          matrix <- new matrix size of (size,1)
          matrixA[i,0] <- y-coordinates[i]*y-coordinates[i]
          matrixA[i,1] <- y-coordinates[i]
          matrixA[i,2] <-1
          matrix[i,0] <-z-coordinates[i]
        End
          Initialize matrixInverse <- Inverse (matrixA)
          Initialize matirxMul <- matrixInverse*matrix
          Initialize a <-  matrixMul(0,0)
          Initialize b <-  matrixMul(1,0)
          Initialize c <-  matrixMul(2,0)
        For i=0 to size do
        Begin
            Initialize Estimatedz <- a* y-coordinates[i]*y-coordinates[i]+b* y-
coordinates[i]+c
        End
End
End
```

Figure 4.6 Algorithm for Curve Estimation

Algorithm: Algorithm for Circle Estimation

Input: 3D data in order to perform circle model estimation

Output: R-square regression values for all slits lines

```
Begin
For j=0 -> size of cross section do
Begin
  Initialize x-coordinates with input data x coordinates
  Initialize y-coordinates with input data y coordinates
  Initialize z-coordinates with input data z coordinates
  Initialize size <- size of input data
  for i=0 -> size do
        Begin
          Initialize matrixA and matrixB
          martixA <- new matrix size of (size,3)
          matrix <- new matrix size of (size,1)
          matrixA[i,0] <- y-coordinates[i]
          matrixA[i,1] <- z-coordinates[i]
          matrixA[i,2] <-1
          matrix[i,0] <-  -(y-coordinates[i]* y-coordinates[i])-(z-coordinates[i]* z-
coordinates[i])
        End
          Initialize matrixInverse <-  Inverse(matrixA)
          Initialize matirxMul <- matrixInverse*matrix
          Initialize centery <-  -matrixMul(0,0)/2
          Initialize centerz <-  -matrixMul(1,0)/2
          Initialize radius  <-  sqrt((pow(centery,2)+pow(centerz,2))+matrixMul(2,0))
          Initialize temp  <-   radius/sqrt((pow(centery,2)+pow(centerz,2))
        For i=0 to size do
        Begin
            Initialize Estimatedy<-  y-coordinates[i]+(( y-coordinates[i]-centery)*temp)
            Initialize Estimatedy<-  z-coordinates[i]+(( z-coordinates[i]-centerz)*temp)
        End
End
End
```

Figure 4.7 Algorithm for Circle Estimation

4.5 Evaluation of System

The proposed system is evaluated by using three-dimensional point cloud data in circle and curve fitting techniques. The evaluation is taken by considering correlation results of actual input data and estimated data. Z coordinate values are used to estimate the curve models because z coordinates just only work to have a curve in the data. Both Y coordinate values and Z coordinate values are applied to estimate the circle model to observe the reflected circumference coordinates of estimated radius and center. There are 30 intervals cross section of RGB-D sensor. The estimated results of cross section 1 are calculated as samples.

4.5.1 Curve Model Fitting Using 3D Data

In the curve fitting, there are many types of curve fitting from input data points. They are linear, polynomial, exponential, and, logarithmic and power approaches to use for curve fitting. Among them, polynomial curve fitting, for two-dimensional estimation of curve, is used to estimate the best fit. The higher polynomial order is necessary in fitting for curve estimation. There is no data restriction which is associated with the curve fit. In order to be the best fit in curve fitting estimation, the polynomial curve estimation is applied to observe the curve of the best fit.

For curve estimation, the homogeneous parameters are used for z coordinates estimation. Z coordinates just work to curve in the input data. Therefore, the estimated results for z coordinates of one cross section is shown in Table 4.1. The correlation result for curve model fitting for one cross section using point cloud data in fitting is shown in Table 4.2.

For the measurement of pig length, the data is separated 30 mm cross sections to perform the length of ear-to-tail position. For length estimation, there are almost same results in measurement. Using the obtained data of pig, the length can be measured by curve fitting technique. The length of pig along the spine is measured through ear-to-tail positon. The estimated value of pig length using pig model was 110 cm. The measurement of pig in manually was 95 cm in the detection of ear-to-tail position. So the discrepancy value of measuring the length of pig is 15 cm.

Table 4.1 Actual and Estimated Z Coordinates for Cross Section 1

No. of Points	Actual y value	Actual z value	Estimated z value
1	55	850	879.210988
2	44	848	885.6470273
3	60	852	878.987522
4	42	853	887.6953683
5	46	857	883.8688869
6	37	861	893.9983487
7	69	869	882.8409433
8	74	877	887.3459885
9	31	877	903.7910805
10	55	884	879.210988
11	58	884	878.8742579
12	48	887	882.3609471
13	50	885	881.123208
14	53	884	879.7732255
15	55	884	879.210988
16	58	885	878.8742579
17	60	885	878.987522
18	63	887	879.6640443
19	41	891	888.8208641
20	43	889	886.6374227
21	56	886	876.6374227
22	47	892	886.656777
…			
75	129	1009	1048.359

However, it cannot say that how much all of the actual z coordinates values and estimated z coordinates values are in correlation with each other. Adjusted R-square regression model is applied to observe their correlation for each cross section.

R-square value is 0.898044 and adjusted R-square value is 0.801032. The adjusted r-square regression cannot depend on the adding variables even if new variable is not very relevant. The estimated values of adjusted r-square can be proved that the correlation is fair for line number 1 because of the presence of noises in the input data. As the result of correlation is the head position of pig. Therefore, the presence of input data has some noise in capturing.

4.5.2 Circle Model Fitting Using 3D Data

In the measurement of circumference, the chest position is calculated using approximated circle at each cross section. The length of circumference behind the forefoot is measured.

In circle model fitting, the homogeneous parameters are used for estimation of center and radius. The data points are detected on circumference of estimated circle using circle geometry. The estimated results for y and z coordinates of cross section number 1 for RGB-D sensor is shown in Table 4.3. The correlation result for circle model fitting for line number 1 using RGB-D sensor is shown in Table 4.4 and Table 4.5.

In the measurement of circumference, the chest position is calculated using approximated circle at each cross section. Three-dimensional data of circumference is shown in appendix figure 6. For the estimation of circumference, the circumference of the chest was approximated by the acquired cross sectional data was 135 cm and the measurement of chest circumference of a pig model with a major was 121 cm. Since the differences of between estimated and actual values was 14 cm occurred. Since the chest circumference of the pig is not a perfect circle, it is considered that a deviation occurred between the diameter approximated by the circle and the value measured by the measurement system. The modelling of pig length and circumference estimation with three-dimensional data is shown in appendix figure 7. Therefore, the measurement of pig weight can be estimated using these two estimation such as the pig length and chest circumference measurements.

Table 4.2 Adjusted R-square Regression Model for Curve Model Estimation of Cross Section 1

No. of Points	z-coordinate	Estimated z-coordinate	For z-coordinate	
			Square ssot	Square sse
1	853.2818199	853.2818199	853.2818199	853.2818199
2	1417.298663	1417.298663	1417.298663	1417.298663
3	728.3263437	728.3263437	728.3263437	728.3263437
4	1203.768583	1203.768583	1203.768583	1203.768583
5	721.9370822	721.9370822	721.9370822	721.9370822
6	1088.891018	1088.891018	1088.891018	1088.891018
7	191.5717109	191.5717109	191.5717109	191.5717109
8	107.0394776	107.0394776	107.0394776	107.0394776
9	717.7619933	717.7619933	717.7619933	717.7619933
10	22.93463594	22.93463594	22.93463594	22.93463594
11	26.27323187	26.27323187	26.27323187	26.27323187
12	21.52081162	21.52081162	21.52081162	21.52081162
13	15.02951621	15.02951621	15.02951621	15.02951621
14	17.8656225	17.8656225	17.8656225	17.8656225
15	22.93463594	22.93463594	22.93463594	22.93463594
	…			
75	1009	1048.359	-39.3592	1549.151
	Sum=68038	Sum=68038	Sum=142866.5	Sum=14566.08
	Mean=919.4324324			
R –square=0.898044				
Adjusted R-square=0.801032				

Table 4.3 Actual and Estimated Y and Z Coordinates for Cross Section 1

No. of Points	y-coordinate	z-coordinate	Estimated y-coordinate	Estimated z-coordinate
1	55	850	63.58926714	875.7654691
2	44	848	57.49332616	878.1393859
3	60	852	66.47823804	874.8753677
4	42	853	55.07166517	879.2830914
5	46	857	56.25950023	878.7070774
6	37	861	49.95346985	882.1182333
7	69	869	70.10506987	873.958449
8	74	877	73.37211957	873.3163788
9	31	877	41.11274555	888.6101174
10	55	884	53.02133054	880.3479707
11	58	884	55.58234584	879.0318495
12	48	887	46.26456276	884.5546241
13	50	885	48.66359907	882.930056
14	53	884	51.40934397	881.2507567
15	55	884	53.02133054	880.3479707
16	58	885	55.14725157	879.2455595
17	60	885	56.96549847	878.37848
18	63	887	59.02235057	877.4778831
19	41	891	39.84623429	889.742278
20	43	889	42.02063739	887.8336557
…				
75	129	1009	119.6686	994.2036

All of the actual y and z coordinates values and reflected y, z coordinates values are in correlation with each other. However, it cannot state that how much

related each other. Therefore, Adjusted R-square regression model is applied to observe their correlation for each cross section.

Table 4.4 Adjusted R-square Regression of Y-coordinates for Circle Model Estimation of Cross Section 1

No. of Points	y-coordinate	Estimated y-coordinate	y-coordinate	
			Square ssot	Square sse
1	55	63.58926714	1.922844444	73.77551
2	44	57.49332616	153.4295111	182.0698508
3	60	66.47823804	13.05617778	41.96756809
4	42	55.07166517	206.9761778	170.8684302
5	46	56.25950023	107.8828444	105.257345
6	37	49.95346985	375.8428444	167.7923811
7	69	70.10506987	159.0961778	1.221179425
8	74	73.37211957	310.2295111	0.394233832
9	31	41.11274555	644.4828444	102.2676226
10	55	53.02133054	1.922844444	3.915132843
11	58	55.58234584	2.602844444	5.845051625
12	48	46.26456276	70.33617778	3.011742408
13	50	48.66359907	40.78951111	1.785967459
14	53	51.40934397	11.46951111	2.530186594
15	55	53.02133054	1.922844444	3.915132843
	…			
75	129	119.8686	5272.696	87.07519
	Sum=4229	Sum=4191.923	Sum = 62605.79	Sum=1728.66
	Mean=56.386667			
R-square=0.972388				
Adjusted R-square=0.944026				

Adjusted R-square value is 0.972388 and adjusted r-squared value is 0.944026. These two values direct to the correlation between actual data and estimated data. The result of r-square and adjusted r-square are almost 1. It is called the best fit in Y-coordinates in circle estimation. One difference between r-square and adjusted r-square model is that r-squared depends on every independent and dependent variables in the model, and adjusted r-squared adjusts the number of predictors in the model. This tends to goodness of fit in analysis. Therefore, estimated y-coordinates of r-square can be proved that the correlation is really good for cross section 1.

R-square value is 0.925812682 and adjusted R-square value is 0.853160486. This value directs to the correlation between actual data and estimated data. The result of r-square and adjusted r-square are almost 1. This tends to goodness of fit in analysis. Therefore, estimated z-coordinates of r-square can be proved that the correlation is best fit for cross section 1.

4.5.3 Experimental Results of Adjusted R-square Regression Model

The calculation of experimental results in this system is just dependent on thirty cross sections for three-dimensional point cloud data of RGB-D sensor. As experimental results, the adjusted R-square Regression value for cross sections are the accuracy results for one portion of measurement target. Three-dimensional data is examined by curve model estimation which is calculated the accuracy between the actual data and estimated data by the adjusted R-square Regression Model. If all the data are nearly 1 in analysis, it is represented as good data for both curve and circle estimation. Therefore, the correlation values of input data and estimated data are shown in Table 4.6 and Table 4.7.

For curve model estimation, it can be said that it can estimate well on all the cross sections position in RGB-D sensor. The correlation values of curve model fitting for sensor are almost stable. Therefore, the values change on cross section 1,2,5,9, 25, 26 and 30. For cross section 26 and 27, the tail position becomes to avoid to fit the curve model because it presence the data of fore legs in pigs and it goes to wrong estimation of curve. Cross section 1, 2 and 5 are the ear position and the reason

that happens insufficient approach to use two-power curve for these line numbers. Therefore, the applied curve model and input data are flexible in this system.

Table 4.5 Adjusted R-square Regression of Z-coordinates for Circle Model Estimation of Cross Section 1

No. of Points	z-coordinate	Estimated z-coordinate	z-coordinate	
			Square ssot	Square sse
1	663.8593991	663.8593991	663.8593991	663.8593991
2	908.3825812	908.3825812	908.3825812	908.3825812
3	523.2824486	523.2824486	523.2824486	523.2824486
4	690.8008954	690.8008954	690.8008954	690.8008954
5	471.1972082	471.1972082	471.1972082	471.1972082
6	445.9797786	445.9797786	445.9797786	445.9797786
7	24.586216	24.586216	24.586216	24.586216
8	13.56906508	13.56906508	13.56906508	13.56906508
9	134.794826	134.794826	134.794826	134.794826
10	13.33731821	13.33731821	13.33731821	13.33731821
11	24.6825191	24.6825191	24.6825191	24.6825191
12	5.979863072	5.979863072	5.979863072	5.979863072
13	4.284668039	4.284668039	4.284668039	4.284668039
14	7.558338845	7.558338845	7.558338845	7.558338845
15	13.33731821	13.33731821	13.33731821	13.33731821
…				
75	1009	994.2036	10368.67	218.9339017
	Sum=68038	Sum=67909.15	Sum=131940.7	Sum=9788.330162
	Mean=907.1733333			
R –square=0.925812682				
Adjusted R-square=0.853160486				

Table 4.6 Curve Model Estimation Accuracy using Adjusted R-square Regression Model for Cross sections

Cross Sections	Adjusted R-square Regression for RGB-D Sensor
1	0.773813
2	0.795558
3	0.902236
4	0.945165
5	0.874319
6	0.974984
7	0.944795
8	0.928625
9	0.712625
10	0.955173
11	0.976170
12	0.983139
13	0.986503
14	0.969375
15	0.980069
16	0.930318
17	0.711469
18	0.332629
19	0.323498
20	0.912255
21	0.970388
…	…
35	0.853380

Table 4.7 Circle Model Estimation Accuracy using Adjusted R-square Regression Model for Cross Sections

Cross sections	R-square Regression for RGB-D Sensor	
	For y coordinates	For z coordinates
1	0.944026	0.853166
2	0.975098	0.944942
3	0.997268	0.931510
4	0.999067	0.979619
5	0.999328	0.906255
6	0.999064	0.995282
7	0.999599	0.997559
8	0.999875	0.997842
9	0.991043	0.795529
10	0.999523	0.978817
11	0.998688	0.984555
12	0.998939	0.991926
13	0.998521	0.990284
14	0.999232	0.990072
15	0.999501	0.994966
16	0.998218	0.996203
17	0.998483	0.995060
18	0.967424	0.957480
19	0.960711	0.678815
20	0.993623	0.243452
…	…	…
35	0.988850	0.872252

Three-dimensional data for curve model estimation is presented in Appendix Figure-3 and Figure-6.

For the depth sensor, it can estimate well on y coordinates. The adjusted r-square values for y coordinates are high and the estimated model is compatible with input data for y coordinates. However, the r-square values of z coordinates get good values from cross section 2 to 25. The others are lower than normal ones because the head position of pig' ears and other noises leads to be inflexible with estimated model to input data. That's why it goes to be low correlation values.

According to correlation results, this system can estimate well on the data with compatible results. However, it is very important to apply the suitable models to fit the input data because the estimated results cannot be flexible with input data. Therefore, the user should understand which models they want to fit the input data and apply the appropriate models to observe the effective correlation values.

CHAPTER 5

CONCLUSION, LIMITATION AND FURTHER EXTENSIONS

5.1 Conclusion

In reconstruction of three-dimensional data of objects, there are many types of RGB-D sensors such as Microsoft KINECT, Asus Xtion 2, and Intel RealSense and so on. These are very popular to reconstruct 3-dimensional data of objects. Using 3D sensors can observe the whole surface of object with a single shot of object. These sensors can also get point cloud data using Time-of-flight and Structured Light Projection Method.

The major aim of the proposed system is to analyze the accuracy results of multiple slits Xtion2 depth sensor for curve, circle model fitting and values of length and girth of pig to accurately obtain and show the accuracy percentages of circle and length of pig measurements. For curve model estimation, 2-power curve, polynomial curve estimation, is applied. For circle model estimation, circle geometry theory is used. R-square regression model is used to verify the correlation between estimated results and real results. Then, the adjusted R-square regression model is also applied to prove the correlation between real results and estimated results. The performance of this system is considered on cross sections of 3D point cloud data. Therefore, x-coordinates are reduced to get each cross section.

In this system, Xtion 2 depth sensor can provide incomplete point cloud data to the shapes of curve and circle model with flexible accuracy results. The results of 30 slits in cross section is that curve and circle model can estimate well along the pig body. However, it cannot estimate well on the slit line number where it projected on tail, head and ear positions of pig because adjusted r-square values verify that the model uses for those slits are incompatible with input data. However, the three-dimensional point cloud data with cross sections can estimate the shape of curve and circle model object well by analyzing these results. This system constructs cross sections by separating x-coordinates horizontally. The main problem in depth sensor is its background. If the background extraction does not work well, many noises

appear in measurement image and it goes down the model fitting correlation results. Therefore, it is very important to apply an effective background extraction procedure to apply the depth sensor and to have accurate correlation results in model fitting procedure.

The most important thing is that the size and shape of the object can influence the accuracy of shape estimation results. Therefore, it is better to apply the most suitable shape estimation procedure for robot vision systems.

The estimated curve and circle can perform the effective goodness of fit using adjusted r-squared regression model. According to the statistical analysis, the goodness of fit can make strong relationship of curve and circle fitting. Therefore, the data are reliable on curve and circle fitting estimation in the case of measuring the length and girth of pig.

5.2 Limitation

The system is only considered for each cross section which plays on the back shape of pig body. The back shape of pig is curve shapes. Therefore, this system cannot be run on the different shapes of object. Depth sensor cannot work for black color objects. It can work well within 8m. Therefore, it is important to consider the limitations of devices to use in real applications.

5.3 Further Extensions

Estimation of other models using this approach and testing with different regression models to determine the correlation between input and estimated data would be further extensions of the system.

REFERENCES

[1] A. Bigdelou, T. Benz, L. Schwarz, N. Navab, "*Simultaneous categorical and spatio-temporal 3D gestures using Kinect",* IEEE Symposium on 3D User Interfaces, Costa Mesa, CA, USA, 2012, pp. 53-60.

[2] Agnes Swadzba, *"Estimation of Camera Motion from Depth Image Sequences",* ME Thesis, Bielefeld University, 2006.

[3] Axelsson, L., Karlsson, N.: "*Object recognition using a laser scanner and fourier-transform"*. Optical Engineering 36(6) (June 1997) 1721-1726.

[4] Brandl N, Jorgensen E. "*Determination of live weight of pigs from dimensions measured using image analysis"* [J]. Computer and Electronics in Agriculture. 1996; 15(1):57-72.

[5] C. Dal Mutto, P. Zanuttigh, G. Cortelazzo, "*Time-of-Flight Cameras and Microsoft Kinect*", Springer Briefs in Electrical and Computer Engineering, 2012.

[6] D. Bhatnagar, A. Pujari, P. Seetharamulu, "*Static scene analysis using structured light",* Image and Vision Computing, Vol.9 , 1991, pp.82-87.

[7] Darwish, Walid et al. "*A New Calibration Method for Commercial RGB-D Sensors*" Sensors (Basel, Switzerland) vol. 17(6) 1204. 24 May. 2017 [online]. Available: https://doi.org/10.3390/s17061204

[8] Doeschl- Wilson A B(2004), Whittemore C T, Knap P W, Schofield C P. "*Using visual image analysis to describe pig growth in terms of size and shape"* [J]. Animal Science. 2004

[9] Florian Faion, Marcus Baum, and Uwe D. Hanebeck, "*Tracking 3D Shapes in Noisy Point Clouds with Random Hypersurface Models"*, 15th International Conference on Information Fusion, Singapore, July 2012.

[10] Gokturk, S.B.; Yalcin, H.; Bamji, C. "*A time-of-flight depth sensor-system description, issues and solutions"*. In Proceedings of the Conference on Computer Vision and Pattern Recognition Workshop, Washington, DC, USA, 27 June–2 July 2004.

[11] Guisser, L., Payrissat, R., Castan, S.: "*A new 3D surface measurement system using a structured light"*. In Computer Vision and Pattern Recognition. (1992) 784-786.

[12] Hamed Sarbolandi, Damien Leoch, and Andreas Kolb. "*Principle of structured light based systems"*. Reproduced as Figure 1 in [23], 2015. [Image].

[13] Hofer, M., Odehnal, B., Pottmann, H., Steiner, T., Wallner, J.: "*3D Shape Recognition and Reconstruction based on line element geometry"*. In Proceeding International Conference on Computer Vision. (2005), Volume II: 1523-1538.

[14] Intel RealSense Technology. (2018, November). Intel Real Sense Depth Sensor [online]. Available: https://en.wikipedia.org/wiki/Intel_RealSense

[15] Je, C., Lee, S., Park, R.: "*High-contrast color-stripe pattern for rapid structured-light range imaging"*. In: European Conference on Computer Vision. (2004) Vol I: 95-107.

[16] Jungong Han; Ling Shao; Dong Xu; Shotton.J ,"*Enhanced Computer Vision With Microsoft Kinect Sensor: A Review*," Cybernetics, Institute of Electrical and Electronics Engineers Transactions on vol.43, no.5, pp.1318, 1334, Oct.2013

[17] Kashiha M. et al. (2014) ,"*Weight Estimation of Pigs Using Top-View Image Processing"*. In: Campilho A., Kamel M. (eds) Image Analysis and Recognition. International Conference on Image Analysis and Recognition 2014. Lecture Notes in Computer Science, vol. 8814. Springer, Cham, 496-503

[18] Lee,K., Je, C., Lee, S.: "*Color-stripe structured light robust to surface color and discontinuity"* In: Asian Conference on Computer Vision. (2007) II: 507-516.

[19] Microsoft Kinect Sensor (2010). *Information of Kinect* [online]. Available: https://developer.microsoft.com/en/windows/kinect

[20] P. Garbat, W. Skarbek, M. Tomaszewski, "*Structured light camera calibration, Opto-Electron*", Review 21(1), 2013, pp.23-38.

[21] P. Lancaster and K. Salkauskas, "*Surfaces generated by Moving Least Squares Methods*", Mathematics of Computation, volume 37, pp. 141-158, July 1981 [online]. Available: http://dx.doi.org/10.1090/S0025-5718-1981-0616367-1

[22] Pottmann, H., Leppoldesder, S., Hofer, M.: *"Registration without Iterative Closest Point"*. Computer Vision and Image Understanding 95(1) (July 2004) pp. 54-71.

[23] Pottmann, H., Hofer, M., Odehnal, B., Wallner, J.: *"Line geometry for 3d shape understanding and reconstruction"*. In Proc. European Conference on Computer Vision. (2004) Vol I: 297-309.

[24] Pottmann, H., Huang, Q., Yang, Y., Hu, S.: "*Geometry and convergence analysis of algorithms for registration of 3d shapes"*. International Journal of Computer Vision (May 2006) 277-296.

[25] Wang, Y, Yang, W., Winter, P., Walker, L (2008), "*Walk-through weighing of pigs using machine vision and an artificial neural network,"* Biosyst.Eng.100(1), 117-12(2008).

[26] Y. Cheng and M. Peng, "*Boundary element-free method for elastodynamics,*" Science in China G:Physics and Astronomy, volume 48, Issue 6, pp. 641-657,2005

[27] Z. Zhang, "*Microsoft kinect sensor and its effect*", Institute of Electrical and Electronics Engineers Multimedia, Vol.19, 2012, pp.4-10.

[28] Z. Komargodski and D. Levin, "*Hermite type moving-least-squares approximations*," Computers and Mathematics with Applications, volume 51, Issue 8, pp. 1223-1232,2006

APPENDIX

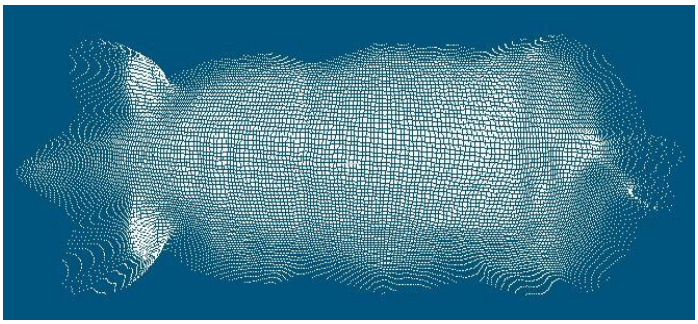

Figure 1 3-Dimensional Image of Pig Model using RGB-D Sensor

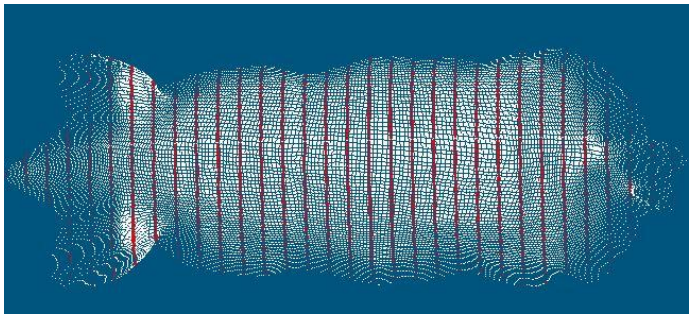

Figure 2 Cross sections 1, 2, 3... 1ith line 30

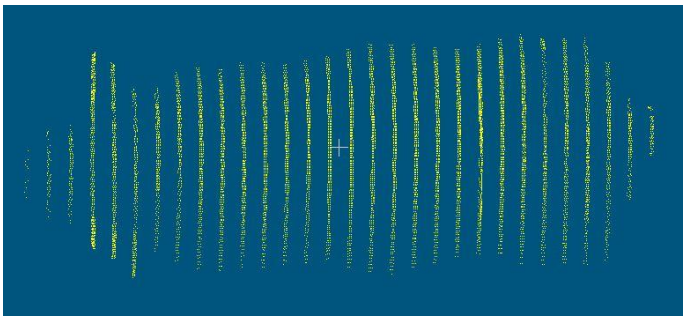

Figure 3 Curve Model Estimation of Pig Model

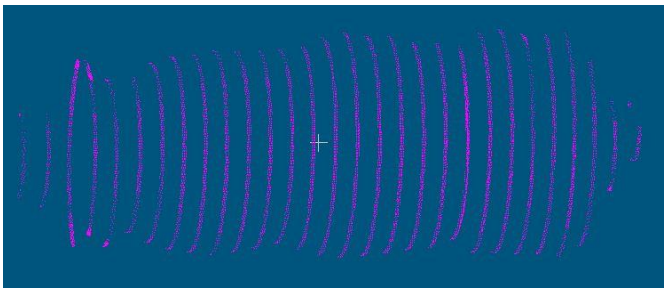

Figure 4 Circle Model Estimation of Pig Model

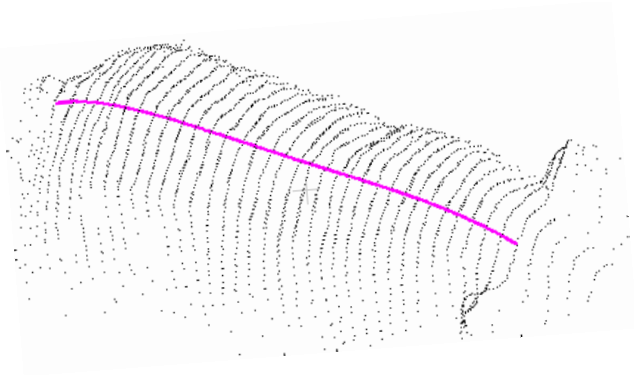

Figure 5 Detection of length in pig model

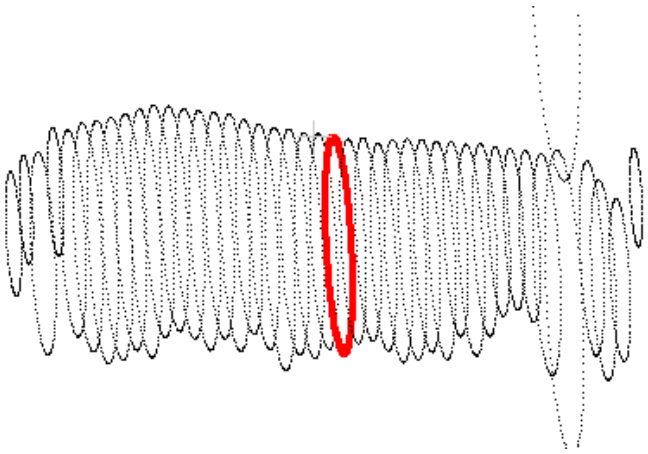

Figure 6 Detection of circumference in pig

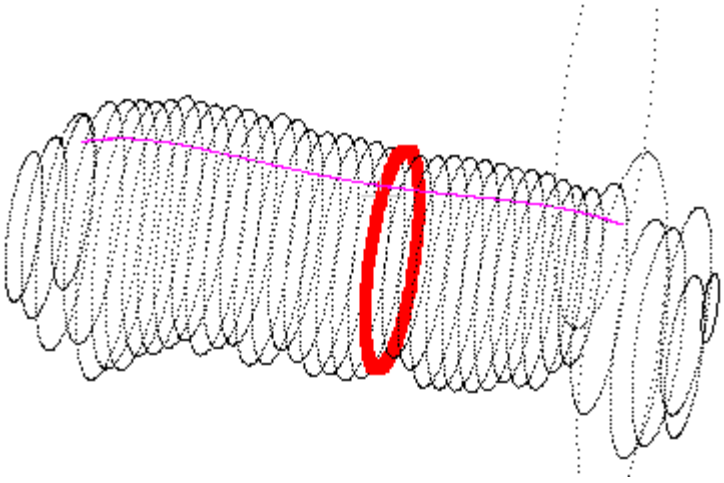

Figure 7 Modelling of Pig measurement